Marine Pollution Bulletin 203 (2024) 116477

Contents lists available at ScienceDirect

Marine Pollution Bulletin

journal homepage: www.elsevier.com/locate/marpolbul

Navigating spatio-temporal microbiome dynamics: Environmental factors and trace elements shape the symbiont community of an invasive marine species

Carles Galià-Camps [a,b,c,*], Liam Junkin [a], Xavier Borrallo [a], Carlos Carreras [a,b,1], Marta Pascual [a,b,1], Xavier Turon [c,1]

[a] Departament de Genètica, Microbiologia i Estadística, Universitat de Barcelona, Avinguda Diagonal 643, 08028 Barcelona, Spain
[b] Institut de Recerca de la Biodiversitat (IRBio), Universitat de Barcelona (UB), Barcelona, Spain
[c] Department of Marine Ecology, Centre d'Estudis Avançats de Blanes (CEAB-CSIC), Accés Cala Sant Francesc 14, 17300 Blanes, Spain

ARTICLE INFO

Keywords:
Styela plicata
Tissue-specificity
Seasonality
Adaptation
Core ASVs
Indicator ASVs

ABSTRACT

The proliferation of marine invasive species is a mounting concern. While the role of microbial communities in invasive ascidian species is recognized, the role of seasonal shifts in microbiome composition remains largely unexplored. We sampled five individuals of the invasive ascidian *Styela plicata* quarterly from January 2020 to October 2021 in two harbours, examining gills, tunics, and surrounding water. By analysing Amplicon Sequence Variants (ASVs) and seawater trace elements, we found that compartment (seawater, tunic, or gills) was the primary differentiating factor, followed by harbour. Clear seasonal patterns were evident in seawater bacteria, less so in gills, and absent in tunics. We identified compartment-specific bacteria, as well as seasonal indicator ASVs and ASVs correlated with trace element concentrations. Among these bacteria, we found that *Endozoicomonas*, *Hepatoplasma* and Rhodobacteraceae species had reported functions which might be necessary for overcoming seasonality and trace element shifts. This study contributes to understanding microbiome dynamics in invasive holobiont systems, and the patterns found indicate a potential role in adaptation and invasiveness.

1. Introduction

Marine invasive species have emerged as a critical concern in the last decades (Roy et al., 2023). These non-native species are capable of reaching widely distant areas aided by human activities. In the new distribution range, the absence of natural predators or competitors, in combination with their intrinsic biological strategies, can allow a fast establishment and the colonisation of new habitats (Sodhi and Ehrlich, 2010). The disruption of locally balanced ecosystems due to the proliferation of invasive species can result in an ecological cascade, including habitat degradation, alteration of food webs, decline of native species, and the introduction of new pathogenic elements into the occupied habitats (Nikolaou et al., 2023; Roy et al., 2023; Walsh et al., 2016). These consequences have direct impacts on the global economy, costing millions of dollars every year in terms of production losses of commercially important species, losses of ecosystem services, costs of eradication of harmful invasive species, and interference with human-made structures (Connelly et al., 2007; Roy et al., 2023; Walsh et al., 2016). To unravel the mechanisms that allow alien species to become invasive, genomics has been pointed out to be one of the most powerful tools, since pre-existing genomic features such as genes responsible for the production of heat shock proteins, or those involved in the immune system or in resistance to pollutants or salinity, may confer these species higher chances to overcome a wide variety of non-native conditions (Galià-Camps et al., 2024; Schrader et al., 2014; Stern and Lee, 2020; Wei et al., 2020).

In addition, symbiotic associations with micro-organisms can also allow invasive species to overcome shifting conditions, since bacterial communities have the potential to change quickly when submitted to varying external conditions and enhance the host fitness over a range of environmental variation (Cheng et al., 2018; Koskella et al., 2017; Villela, 2020). Organisms should be viewed as holobionts (hologenomes in

* Corresponding author at: Departament de Genètica, Microbiologia i Estadística, Universitat de Barcelona, Avinguda Diagonal 643, 08028 Barcelona, Spain.
E-mail addresses: cgaliacamps@gmail.com (C. Galià-Camps), liam.junkin@gmail.com (L. Junkin), carreras@ub.edu (C. Carreras), martapascual@ub.edu (M. Pascual), xturon@ceab.csic.es (X. Turon).
[1] Senior author.

https://doi.org/10.1016/j.marpolbul.2024.116477
Received 26 November 2023; Received in revised form 30 April 2024; Accepted 6 May 2024
Available online 16 May 2024

genetic terms), understood as the integration of both microbiome and their host as a living ecological and evolutionary unit (Baedke et al., 2020; Rosenberg and Zilber-Rosenberg, 2018; Singh et al., 2020). From this perspective, rich microbiomes have previously been employed as proxies for predicting the success of invasive species. This is because they imply the presence of a diverse reservoir of microbial variation that can be utilised to finely adjust adaptive responses, thereby aiding in the colonisation of new environments (Dragičević et al., 2021; Goddard-Dwyer et al., 2021). Microbiome adjustment can occur at a temporal scale that is almost instantaneous compared to other adaptive processes that occur over host generations, and these microbiome changes are thus potentially important for the introduction success.

Among invasive species with rich microbiomes, ascidians have emerged as a group of relevant interest since they have been repeatedly shown to include an unexpected spatio-temporal and tissue-specific diversity of symbionts with possible implications in the host fitness (Dror et al., 2019; Evans et al., 2017; López-Legentil et al., 2023; Utermann et al., 2020). Furthermore, a recent study performed on the ascidian *Styela plicata* demonstrated the presence of ontogenetic changes in microbiomes, in which the tissue-specific bacterial communities were more similar to that found in the surrounding seawater in early life stages, but developed into well-differentiated communities in adults (Galià-Camps et al., 2023). The interplay between extremely rich microbiomes and the genomic plasticity of ascidian hosts has enabled several ascidian species to colonise artificial structures such as shellfish rafts and harbours worldwide (Casso et al., 2020). In these structures, ascidians cause important economic losses, since they compete for feeding resources against other filtering species of commercial interest such as mussels or oysters, or by fouling boat hulls and increasing their fuel consumption when navigating (Aldred and Clare, 2014).

In the present scenario of increasing invasion pressure as a consequence of climate change, globalisation, and an increase in transoceanic transport, anthropogenic structures act as marine invasive species hotspots since they offer shelter to those species that arrive from distant habitats attached to ship hulls and in ballast waters (Borden and Flory, 2021; Ferrario et al., 2017; Roy et al., 2023), and this applies particularly to ascidians (López-Legentil et al., 2015). This fact is paradoxical, as harbours are also subjected to harsh conditions such as high pollutant concentrations and extreme seasonal regimes due to shallow depths and isolation from open waters, which accentuate temperature and salinity shifts (Chen et al., 2020; Tamburini et al., 2020). Although the latter factors are somehow predictable and seasonal shifts are progressive, this is not the case for anthropic pollutants, whose concentrations are tied to human activity, and therefore, sudden changes in water conditions can occur. Abrupt environmental changes are a major threat to living organisms since, usually, the host's genomic machinery is unable to provide a fast response to ensure the individual's survival (Han et al., 2023; Rodríguez-Martínez et al., 2019). Thus, microbiome communities can play a prevalent role in the species' resilience to pollutants through fast detoxification (Dearing et al., 2022; Rizvi et al., 2022), and to environmental factors such as temperature or salinity by catalysing some host metabolic activities which allow starving seasons or transitions from the sea to river streams, among others (Lindsay et al., 2020). For *Styela plicata*, it was demonstrated that different tissues bioaccumulate pollutants differentially. The microbiome composition of the gills was correlated with environmental zinc levels, while tunic microbiomes correlated with high concentrations of several elements such as aluminium, iron, and arsenic (Galià-Camps et al., 2023). In addition, most studies on the relationship between microbial composition and environmental stressors in ascidians cover a single or a few time-points, and only Dror et al. (2019) have considered a temporal perspective over seasons.

In this work we analysed bacterial 16S amplicon sequences of different adult compartments (tunic and gills) of the introduced solitary ascidian *Styela plicata*, together with water samples, collected quarterly over two years in two different harbours where we also monitored environmental conditions (temperature and trace element concentrations). We assessed the microbiome shifts of an invasive marine species in terms of diversity and community structure through a multidimensional approach encompassing the influence of the biosphere, the hydrosphere, and the anthroposphere. This study contributes to setting the stage for the understanding of adaptation in invasive marine species' holobionts and how these units change through time and space according to the surrounding conditions.

2. Material and methods

2.1. Sampling and field procedures

From January 2020 to October 2021, we sampled every three months 5 adult individuals of *Styela plicata* (defined as having >40 mm in length) from the harbours of Blanes and Vilanova i la Geltrú in the NW Mediterranean (Fig. A.1, Table A.1). The harbour of Blanes (41.6739 N, 2.7987 E) is a leisure/fishing port characterised by its small size and relatively clean waters, with a wide mouth that allows seawater admixture between the inner harbour and the open sea. On the other hand, Vilanova i la Geltrú (from now on Vilanova, 41.2144 N, 1.7354 E) is a bigger harbour encompassing fishing, commercial, and leisure activities. It has many docks that hinder seawater exchanges (Table A.1). Individuals, fouling ropes from 0 to 1 m depth, were collected by hand by pulling ropes. All individuals were collected on different ropes situated at least 5 m away from each other in order to reduce potential genetic relatedness among them. Right after collection, individuals were immediately photographed on a gridded petri dish for size measurement and sagittally dissected (Fig. A.1). The left half was preserved in glass vials filled with ethanol 96 %, which was repeatedly changed to ensure dehydration of the tissues and posteriorly stored at 4 °C until DNA extraction. The right half was immediately snap-frozen in liquid nitrogen inside 8 mL plastic vials and kept at −80 °C for future studies. Furthermore, 4 surface seawater samples of 250 mL each were collected in previously autoclaved glass bottles at the same sampling dates. Three of them were intended for microbiome analyses, whereas the fourth one was transferred to 100 mL plastic vials and frozen at −20 °C for trace element quantification.

2.2. Laboratory sample processing

For each ethanol-preserved ascidian, we excised a tissue sample from the tunic and the gills, as these two compartments have a highly distinct microbial community in *S. plicata* (Galià-Camps et al., 2023). For the tunic, we first removed the outer layer in contact with the environment and the soft layer in contact with the organism mantle to avoid non-tunic symbionts, and we cut a square of approximately 5 × 5 mm and a thickness of 2–3 mm with disposable scalpels. For gills, a single branchial fold was extracted using sterile tweezers. We conducted tissue DNA extractions with the Puregene® Core Kit B following the manufacturer's January 2022 version instructions (QIAGEN, Valencia, USA). Alongside the ascidian samples, five negative controls in total were processed following the same extraction protocol without adding any tissue. Seawater samples intended for microbiome analyses were filtered through a 47 mm diameter, 0.2 μm pore-size polycarbonate sterilised filter (Merck Millipore, Tullagreen, IRL) under a laminar flow hood to avoid contamination. The filter was stored at −80 °C until DNA extraction. Half of the filter was enzymatically digested with proteinase K and a custom homogenization buffer containing Tris-Cl, EDTA, NaCl, and SDS. DNA was posteriorly isolated following the phenol-chloroform protocol (Galià-Camps et al., 2023). As before, a total of five negatives for water were obtained by processing clean, unused filters.

The V4 region of the 16S rRNA gene was amplified using the primers F515/R806 (Caporaso et al., 2011). All Polymerase Chain Reactions (PCRs) were carried out with 15 μL of Phusion® High-Fidelity PCR Master Mix (New England Biolabs, Beijing, China), 0.2 μM of each

forward and reverse primers, and ~ 10 ng of template DNA. PCRs consisted of an initial denaturation step at 98 °C for 1 min followed by 30 cycles of denaturation at 98 °C for 10 s, annealing at 50 °C for 30 s, and elongation at 72 °C for 30 s. A final extension of 5 min at 72 °C was added to the PCR program to ensure complete amplification. Individual Illumina barcodes were attached to each sample. Six PCR negative controls were run during the amplification step without addition of DNA template. PCR amplicons were pooled at equivalent concentrations, end-repaired, A-tailed, and ligated with Illumina adaptors for sequencing. The resulting library was sequenced on an Illumina NovaSeq 6000 partial run, generating 250 bp paired-end reads. The amplification, library preparation, and sequencing were performed by Novogene Co. Ltd. (UK Cambridge Sequencing Center).

2.3. Environmental data quantification

For seawater samples intended for trace element (TE) concentration, we transferred 50 mL of each seawater sample into an independent plastic vial, to which we gently added 95 % nitric acid (HNO_3) to reach pH = 1 before preservation at −20 °C. To measure TE concentration, we thawed the samples and diluted the solutions at a 1:200 ratio with ultrapure water to reduce salt concentration, which could damage the quantification device and hamper the measurements. Seawater sample densities were calculated before the analysis, and TE concentrations were obtained in a NexION350D ICP-MS (inductively coupled plasma mass spectrometry) spectrometer at the Metal Analysis Unit of the Scientific and Technological Services of the University of Barcelona (CCiT-UB). The same procedure was conducted for one negative blank sample, including only ultrapure water. We selected 9 TEs for quantification: vanadium (V), aluminium (Al), iron (Fe), zinc (Zn), arsenic (Ar), lead (Pb), boron (B), copper (Cu) and selenium (Se) for comparison with previous studies (Galià-Camps et al., 2023). Results were transformed to ppb relative to sample volume, and blank values were subtracted from seawater values. Occasionally, this resulted in small negative values, which were transformed to zero. Additionally, for both harbours, we obtained over the duration of the study mean daily seawater temperatures from logger readings (HOBO$^{(R)}$ Pendant Logger). Loggers were attached to ropes at 1 m depth and continuously submerged.

2.4. Read processing and ASV table obtention

We analysed a total of 210 samples altogether, 50 corresponding to seawater, 81 to gills, and 79 to tunics (Table A.2), as two tunic samples (BLA245 and VIL206) failed during the sequencing process. Negative samples and PCR controls did not amplify, indicating no contamination, and therefore were not further processed. Raw sequences were deposited in NCBI under Bioprojects PRJNA982737 (previously used in Galià-Camps et al., 2023) and PRJNA1030313. Note that all sequences came from the same dataset and were analysed together, but were deposited in two different Bioprojects to match the publications' scheme. Reads were assigned to samples based on their unique barcodes and truncated by cutting off the barcode and primer sequences. FLASH (Magoč and Salzberg, 2011) was used to merge the paired reads. Then, fastp software was used to perform quality control of the reads. Chimeric reads were removed with UCHIME (Edgar et al., 2011), using as a reference the ribosomal RNA sequence database SILVA-v138.1 (Quast et al., 2013). Finally, the DADA2 software (Callahan et al., 2016) was used to denoise the reads and obtain the final ASV (Amplicon Sequence Variant) table. DADA2 was performed on merged reads following (Antich et al., 2021). These authors formally compared the use of DADA2 before and after merging and found that the latter was computationally more efficient and retained more low abundance ASVs as correct due to a high confidence on the overlapping bases. These ASVs are missed if sequences are denoised before merging. Furthermore, a high correlation of error rates in the forward and reverse reads was detected. The ASVs were taxonomically assigned with the plugin 'classify-sklearn' of QIIME2 (Hall and Beiko, 2018) using the SILVA-v138.1 database. We used the 2022 International Code of Nomenclature of Prokaryotes (Oren et al., 2023). ASVs that could not be assigned at the Class level or lower were placed in the "Indeterminate" category. Finally, singleton sequences and sequences not being assigned to bacteria were discarded. The final table for downstream microbiome analyses consisted of the abundance (in number of reads) per sample of each ASV and its taxonomic assignment.

2.5. Microbial community analyses

To check sequencing coverage for all samples, we obtained rarefaction curves with the function 'rarecurve' of the R package vegan v2.6–4 (Oksanen et al., 2013), and verified that an asymptote in the number of ASVs was reached at the sequencing depth obtained for all samples. Unless explicitly stated, we conducted microbial community analyses with a non-rarefied ASV relative frequency table in R with the package vegan, and obtained the graphs with the R package ggplot2 v3.4.1 (Wickham et al., 2016).

Samples were treated at the Class taxonomic level. The least abundant Classes whose sum of relative abundances were below 5 % were assigned to the category "Other". The distribution of Classes in the samples was visually represented using the function 'chordDiagram' from the R package circlize v0.4.15 (Gu et al., 2014). To assess diversity, we first calculated ASV richness using a rarefied table, setting the number of reads equal to the sample with lower coverage, corresponding to the sample VIL285T (from Vilanova) with 18,765 reads. Furthermore, we assessed with the same table the Shannon diversity Index with the function 'diversity'from the vegan package. We conducted General Linear Models (GLMs) for both diversity metrics to evaluate differences among the factors: Compartment (Gill, Tunic, Water), Locality (Blanes, Vilanova), Period (Cold, Warm), and their interactions. Samplings in which seawater temperature was below 17 °C (Winter and Spring) were assigned to the category "Cold" and the ones above 19 °C (Summer and Autumn) to "Warm". We fitted the GLMs using the function 'glm' of the package stats v4.2.2, calculated each GLM coefficient of determination (R^2) with the package rsq v2.5 (Zhang, 2018), and performed pairwise comparisons of the significant factors (with a significance cutoff threshold of 0.05) with the package emmeans v1.8.5 (Lenth et al., 2020). We tested the normality of the data with the function 'shapiro.test' from the R package stats and, if failed, a log10 transformation of the data was applied. Homoscedasticity was assessed with a Breush-Pagan test (Breusch and Pagan, 1979) using the function 'bptest' from the R package lmtest v0.9–40 (Torsten et al., 2012).

To evaluate the differences among samples in terms of microbiome composition, we constructed a Bray Curtis (BC) dissimilarity matrix based on the ASV relative frequency with the function 'vegdist' and used it to conduct a non-metric multidimensional scaling (nMDS) plot with the function 'metaMDS'. We hierarchically repeated the analysis for each major group found in the previous nMDS to further evaluate differences within seawater, tunic, and gill samples (see results). Permutational multivariate analyses of variance (PERMANOVA) were conducted for the BC distance matrix including all samples, and for the BC distance matrices including seawater samples, tunic samples and gill samples separately to test the factors Compartment (Gill, Tunic, Seawater), Locality (Blanes, Vilanova), Period (Cold, Warm), and their interactions. We performed PERMANOVA with the function 'adonis2' of vegan, and pairwise comparisons of the significant factors (with a significance cutoff threshold of 0.05) were done with the function 'pairwise.adonis2' implemented in the package pairwiseAdonis v0.4.1 applying a *p*-value adjusted with the Benjamini-Yekutieli correction (Martinez Arbizu, 2020). Homogeneity in dispersion values for each factor was tested using the function 'permutest(betadisper())' from the R package vegan.

2.6. Core and indicator ASVs

We inferred the core, defined as the set of ASVs consistently present on a group of samples, of different bacterial communities with the function 'core_members' of the R package microbiome v1.23.1 (Lahti and Shetty, 2012-2019). We set the parameter detection threshold as 1×10^{-13} relative abundance and the parameter 'prevalence' as 0.95 to identify the cores. A graphical representation of the cores and their detection thresholds with the number of samples was plotted using the function 'plot_core' from the same package. Shared ASVs among cores were identified and represented as an upset plot with the function 'upset' of the package UpSetR v1.4.0 (Conway et al., 2017). Furthermore, we identified indicator ASVs associated with (a) each compartment and (b) each compartment and period using the function 'multipatt' implemented in the R package indicspecies (De Cáceres and Legendre, 2009), with 999 permutations for statistical analyses. In order to keep only those indicator ASVs with the strongest indicator signal, we selected those ASVs in which at least 70 % of the reads belonging to that ASV (parameter B $\geq$ 0.7) were found in at least 70 % of the corresponding samples (parameter A $\geq$ 0.7). Indicator ASVs found for different groups were plotted as Venn diagrams using the function 'venn.diagram' from the package VennDiagram v1.7.1 (Chen and Boutros, 2011). Furthermore, the relative abundance of ASVs found to be indicators of ascidian tissue and period were graphically represented over the two-year sampling time frame, together with their relative abundance in seawater, using ggplot2.

2.7. Environmental variables and associated microbiome

Trace element (TE) concentrations at each locality were graphically represented with barplots using ggplot2. We tested overall pairwise Pearson correlations of the different TEs using the function 'pairs.panels' from the R package psych v2.3.6 (Revelle, 2015). TE values were standardised considering the mean and standard deviation across all samples, regardless of site and season, using the formula ((value-mean)/sd) with the function 'data. Normalization' from the R package clusterSim v0.51–3 (Walesiak et al., 2014). Two-sided paired *t*-tests were conducted between localities for all TE concentrations (averaged over time) with the function 't.test' from the R package stats v4.3.1. To characterise the different samples according to TE concentrations, we performed a Principal Components Analysis (PCA) of the data using the function 'princomp' from the R package stats, and results were graphically represented using ggplot2. To identify potential associations between tissue-specific microbiomes and TEs, we conducted Redundancy Analyses (RDA) using the function 'rda' from the R package calibrate (Graffelman and van Eeuwijk, 2005) and graphically represented the first two axes and TE vectors with ggplot2. The significance of the axes was assessed with the function 'anova.cca', and we identified outlier ASVs whose absolute loadings for the significant axes were higher than the mean value plus 3 times the standard deviation. We retrieved the correlation of each outlier ASV with each TE vector and kept the TE with the highest correlation.

3. Results

3.1. Microbiome community

The initial number of reads was 18,383,866 of which, after the filtering steps, 15,091,572 were retained (Table A.2). The mean number of reads per sample was 71,864.6 ± 11,270.6 (mean ± SD), distributed across 33,634 ASVs (Table A.3). A total of 12,338 ASVs were found in seawater, 22,203 in tunic, and 16,685 in gills (Table A.3). Rarefaction curves showed that all samples reached an asymptote, and therefore the sequencing depth was deemed appropriate (Fig. A.2).

Both localities behaved similarly in terms of ASV distribution at the Class level. Alphaproteobacteria ASVs were prevalent in tunic samples from both localities, especially for Vilanova, and were also highly abundant in seawater samples (Fig. 1a, Table A.4). Seawater samples were also characterised by the presence of Alphaproteobacteria, although they also had a high proportion of Gammaproteobacteria. Gill samples had a high abundance of Indeterminate ASVs, which were practically absent in seawater or tunic (Fig. 1a, Table A.4). Furthermore, gills from Blanes had abundant Bacteroidia ASVs, which were even more abundant in seawater samples. Conversely, Vilanova gill samples had a low abundance of Bacteroidia ASVs (Fig. 1a, Table A.4). Cyanobacteriia were also relatively abundant in seawater samples from both localities and also noticeable in the tunic of individuals from Blanes. The remaining taxonomic Classes considered (Bacilli, Planctomycetia, Actinomycetia, Verrucomycetia, and Others) were not evenly distributed among samples from both localities, although overall they presented low abundances (Fig. 1a, Table A.4).

The Shannon diversity Index and the ASV richness had similar trends for each compartment, although slight differences were found depending on the locality being analysed (Fig. 1b). For the Shannon diversity Index, both localities presented the highest values for seawater (mean value = 4.69) and the lowest for gills (mean value = 2.68), with significant differences between compartment, locality, and their interaction ($p < 0.001$) (Table 1). The tunic displayed different Shannon diversity values depending on the locality (Fig. 1b), being significantly higher for Blanes than for Vilanova ($p < 0.001$, Table A.5). ASV richness responded similarly, although tunic ASV richness in Blanes (mean value = 1271 ASV) was significantly higher than for seawater (mean value = 768 ASVs, $p = 0.004$, Table A.5). Vilanova diversity values were, for both metrics, smaller than in Blanes in all compartments (Table A.5) and significantly different for tunics ($p < 0.001$) and in richness for gills ($p = 0.03$) (Table A.5). When splitting the data into the eight temporal sampling points, as per season and year (Fig. 1b), gill samples had more marked diversity shifts along the seasons than the other compartments. However, patterns were not repeated over the two years surveyed (Fig. 1b). Neither Period (cold or warm) nor any of the interactions involving this factor were significant for both diversity measures (Table 1). In Blanes, tunic diversities remained always high, unlike in Vilanova where temporal shifts were found, although values were always lower than those found in Blanes (Fig. 1b). Finally, seawater samples in Blanes presented consistent seasonality over both years for the Shannon diversity Index and ASV Richness. In Blanes, richness declined from winter to spring, and slowly increased afterward until the year maximum in winter again, while the Shannon diversity Index was higher in the two warmer periods (Fig. 1b). This trend was not found in Vilanova, where the Shannon index and ASV richness varied through time with no clear periodic pattern (Fig. 1b).

When considering the relative abundance of the ASVs found in each compartment in a nMDS plot based on Bray-Curtis dissimilarity (Fig. 2a), a clear distinction between compartments was apparent, with seawater, tunic, and gill samples forming separate groups along the first axis, albeit with some overlap between the ascidian compartments. All factors included in the global PERMANOVA analyses were significant, as well as the double and triple interactions (Table 2). The pairwise analysis of the triple interaction resulted in all comparisons being significant except tunic samples between cold and warm periods in both Blanes and Vilanova ($p = 0.054$ and $p = 0.567$, respectively) (Table A.6). We decided to split the dataset according to compartment since it was the factor with the highest Sum of Squares value (Table 2). For seawater, both locality and period, as well as their interaction, were significant, with similar relative importance for both locality and period, as was apparent in the nMDS with only seawater samples (Fig. 2b, Table 2). The pairwise PERMANOVA tests on the interaction resulted in significant differences among all the comparisons (Table A.7). On the other hand, for tunic samples, only the locality factor was significant (Table 2). The nMDS showed a separation of the two localities, with little overlap (Fig. 2c). Finally, for gills, both factors and their interaction were significant, with locality having a higher importance than period (Table 2).

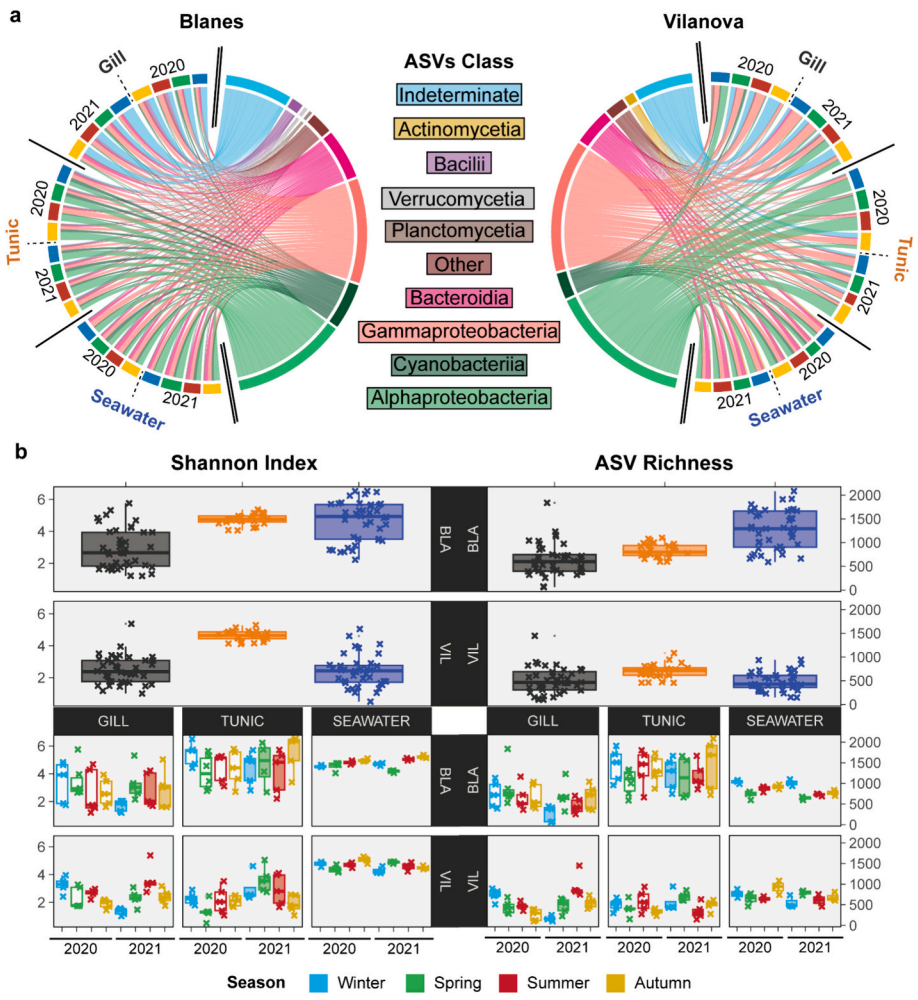

Fig. 1. Composition and diversity of each compartment, locality, and temporal sampling point. **a)** ASV class-level relative abundance in each locality (Blanes and Vilanova). The inner part of the plot indicates the different ASV class-level categories. The outer part shows the samples organized according to compartments (Gill, Tunic, and Seawater) and the eight sampling points. **b)** Shannon diversity Index and Richness values per compartment in each locality based on ASV frequency (upper panels) and separated by the eight temporal sampling points along the two sampling years (lower panels).

Table 1
General Linear Model (GLM) results of the Shannon and Richness values.

Metric	Factors	DF	Sum Sq	F	p-value	R^2
Shannon	Compartment	2	2.37	51.84	**<0.001**	0.215
	Locality	1	1.00	43.65	**<0.001**	
	Period	1	0.00	0.15	0.696	
	Compartment*Locality	2	0.94	20.54	**<0.001**	
	Compartment*Period	2	0.02	0.41	0.662	
	Locality*Period	1	0.01	0.33	0.568	
	Compartment*Locality*Period	2	0.06	1.36	0.260	
	Residuals	198	4.54			
Richness	Compartment	2	1.78	20.26	**<0.001**	0.139
	Locality	1	2.56	58.40	**<0.001**	
	Period	1	0.01	0.23	0.634	
	Compartment*Locality	2	1.36	15.51	**<0.001**	
	Compartment*Period	2	0.08	0.86	0.423	
	Locality*Period	1	0.01	0.17	0.678	
	Compartment*Locality*Period	2	0.13	1.44	0.240	
	Residuals	198	8.68			

Note that Richness values were squared root transformed. As fixed factors we included Compartment (Seawater, Tunic, and Gill), Locality (Blanes and Vilanova), and Period (Cold and Warm). For each factor and its interactions, we provide its degrees of freedom (DF), sum of squares (Sum Sq), F value, and *p*-value. The model adjustment (R^2) is also provided. Significant *p*-values are in bold (threshold <0.05).

Little structure, however, was apparent in the nMDS plot, with samples from different seasons and localities overlapping (Fig. 2d). Nonetheless, for gills, all pairwise comparisons for the interaction were significant (Table A.7).

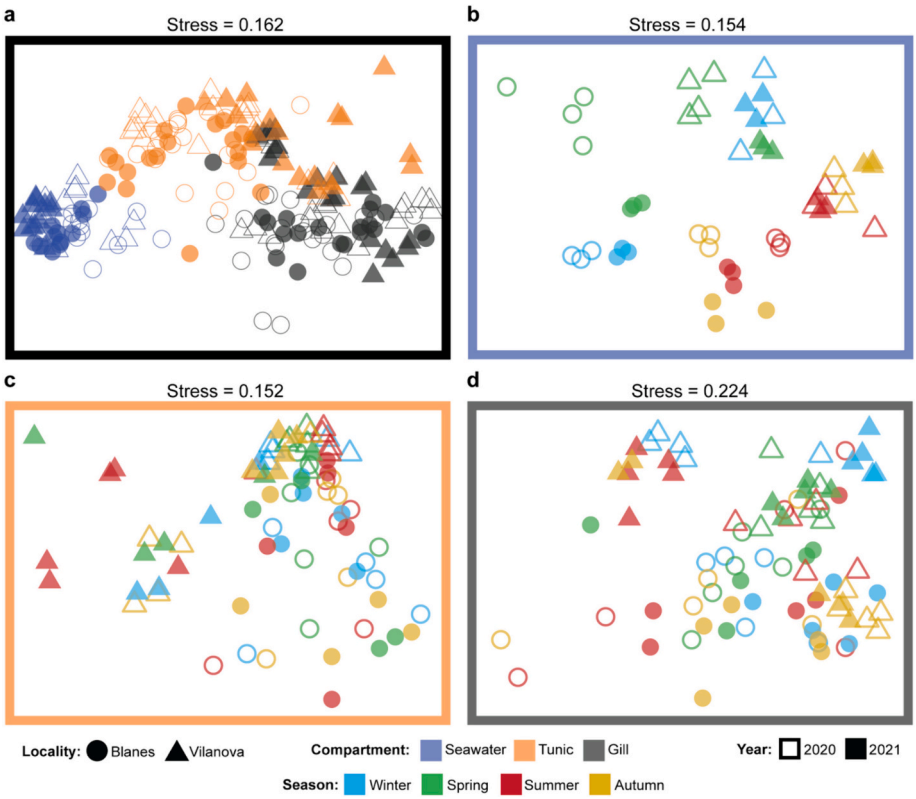

Fig. 2. Microbiome composition dissimilarity over time. **a)** Bray Curtis dissimilarity nMDS plot including all samples. Separate plots were done for **b)** seawater samples, **c)** tunic samples, and **d)** gill samples.

Table 2
PERMANOVAs of the microbiome community defined with Bray-Curtis distance using all samples and each compartment independently.

Compartment	Factor	DF	Sum Sq	R^2	F	p-value
All	Compartment	2	21.41	0.28	49.67	**0.001**
	Locality	1	3.43	0.05	15.92	**0.001**
	Period	1	1.21	0.02	5.61	**0.001**
	Compartment*Locality	2	3.22	0.04	7.47	**0.001**
	Compartment*Period	2	2.06	0.03	4.78	**0.001**
	Locality*Period	1	0.79	0.01	3.65	**0.002**
	Compartment*Locality*Period	2	1.25	0.02	2.90	**0.001**
	Residual	198	42.67	0.56		
Seawater	Locality	1	1.90	0.19	15.12	**0.001**
	Period	1	1.73	0.17	13.73	**0.001**
	Locality*Period	1	0.68	0.07	5.37	**0.001**
	Residual	46	5.79	0.57		
Tunic	Locality	1	2.50	0.12	10.11	**0.001**
	Period	1	0.32	0.01	1.29	0.195
	Locality*Period	1	0.28	0.01	1.14	0.298
	Residual	75	18.58	0.86		
Gill	Locality	1	2.24	0.10	9.42	**0.001**
	Period	1	1.22	0.05	5.15	**0.001**
	Locality*Period	1	1.08	0.05	4.54	**0.001**
	Residual	77	18.29	0.80		

The fixed effects tested (when included) are Compartment (Seawater, Tunic, and Gill), Locality (Blanes and Vilanova), and Period (cold and Warm). For each factor and its interactions, we provide its sum of squares (Sum Sq), degrees of freedom (DF), R^2, pseudo-F (F), and p-value. Significant p-values are in bold (threshold <0.05).

3.2. Core and variable microbiome community

No ASV was present in 100 % of the samples, and neither were 100 % compartment-specific ASVs detected. With the 95 % threshold, ASV76 (*Staphylococcus* sp.) was the only core symbiont across all samples. Following this threshold, a total of 45 ASVs constituted the core community for seawater samples, 4 ASVs for the tunic samples, and 9 for the gill samples (Fig. A.3). When considering only cold water periods, 67 ASVs were core community in seawater samples, 2 for the tunic, and 10 for the gills (Fig. A.3). For the warm period, 76 ASVs comprised the core community for seawater samples, 6 for the tunic, and 12 for gills (Fig. A.3). Although these ASVs were present in 95 % of samples in each group, their abundances were highly variable. Only ASV7, a bacterium from the family Rhodobacteraceae, had a mean abundance above 2 % in the 95 % seawater samples core, whereas other ASVs had abundances mostly below 0.5 % (Table A.3, Fig. A.3). Similarly, for tunic samples only ASV0 (*Methyloceanibacter* sp.) had relatively high abundances (27.9 % of reads), while it was below 0.5 % for all other ASVs (Table A.3,

Fig. A.3). Finally, ASV1 (Gammaproteobacteria), ASV2 (Indeterminate), ASV3 (Indeterminate), had high abundances in the gill core microbiome (14.3 %, 11.6 %, and 12.8 %, respectively), while ASV5 (*Endozoicomonas* sp., 3.3 %) and all other ASVs had lower abundance (Table A.3, Fig. A.3). Only a few ASVs from warm seawater (31 ASVs), cold seawater (23 ASVs), and warm gills (3 ASVs) were found to be private cores, defined as being present only in the core of a single group of samples (Fig. 3a). Seawater cores, considering both temperature periods and overall, shared 40 core ASVs (Fig. 3a). Five core ASVs were shared among gills during both temperature periods (Fig. 3a). Moreover, 12 ASVs were shared between two or more compartments and periods.

When considering the indicator species analyses, many ASVs were significantly associated with each compartment (Supplementary Spreadsheet 1). Seawater had the highest number of indicator ASVs (1816), followed by tunic samples (1551) and gill samples (358). When the indicator species analysis was performed on the dataset split by warm and cold periods, the warm period had more indicator ASVs for the seawater and gills than the cold period (449 vs. 291 and 409 vs. 223, respectively). In contrast, this pattern was reversed for tunics (328 ASVs for the cold period and 247 ASVs for the warm period). When keeping only indicator ASVs in which 70 % of the reads were present in at least 70 % of the samples (Fig. 3b), the number of indicator ASVs dropped to 126 for seawater, 2 for tunic, and 6 for gills (Supplementary Spreadsheet 1). When considering only the cold period, we found 57 indicator ASVs for seawater, 4 for tunic, and 4 for gill (Fig. 3b). For the warm period, 112 ASVs were indicator of seawater, 2 of tunic, and 5 of gills.

Likewise, there were few (cold period) or none (warm period) indicator ASVs shared between compartments (Fig. 3b). The relative abundance values of the indicator ASVs associated with warm and cold periods for the ascidian compartments (tunic and gills) showed that most of them appeared decoupled from the relative abundance trends found in water over time (Fig. 4). Nevertheless, ASV52 and ASV772 both appeared to fluctuate parallelly between tunic and seawater, with increases during the cold periods. On the other hand, ASV4 and ASV8 (with increases in cold periods) and ASV117 (increasing in warm periods) also showed similar abundance trends in gills and water samples (Fig. 4). Interestingly, some tissue indicator ASVs were more abundant in seawater. This is the case of ASV17, ASV7, and ASV64 in tunic samples, and ASV7 in gill samples (Fig. 4).

3.3. Environment-microbiome associations

Trace element (TE) concentrations were highly variable across our temporal samples (Table A.8). Boron was the most abundant (3796.06 ± 660.42 ppb), followed by zinc (20.34 ± 25.68 ppb), while lead was the element with lower values (0.53 ± 0.59 ppb) (Fig. 5a, Table A.8). Trace element concentrations were not highly correlated, except for aluminium with iron, and arsenic with boron, with correlation

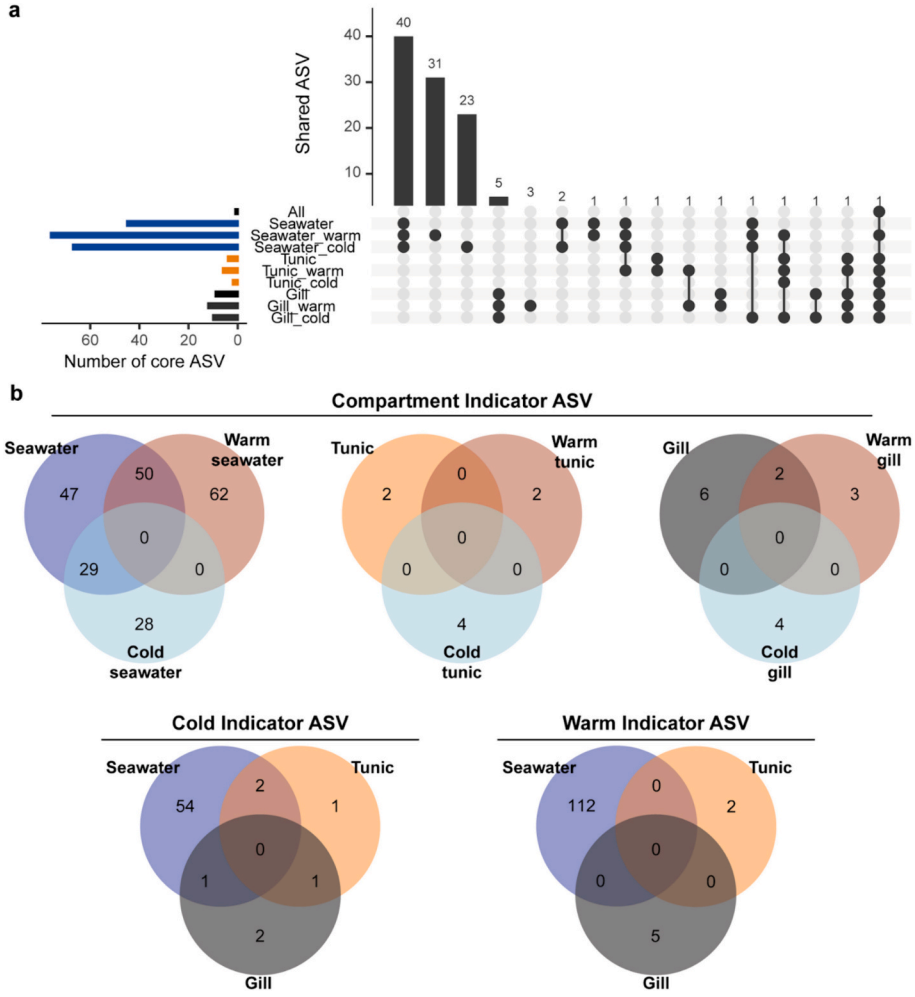

Fig. 3. Compartment 95 % core and indicator ASVs. **a)** 95 % core ASVs for different groupings: all samples combined, for each compartment and for each compartment during cold and warm periods. Coloured horizontal bars represent the number of ASVs found to be core for each group. Vertical bars represent the number of core ASVs specific to a group or shared among them. Dots identify in which groups the ASVs represented in each vertical bar are found. **b)** Venn diagrams of the number of indicator species (ASVs whose 70 % of total reads are present in 70 % of the samples of each group) across combinations of compartment and period.

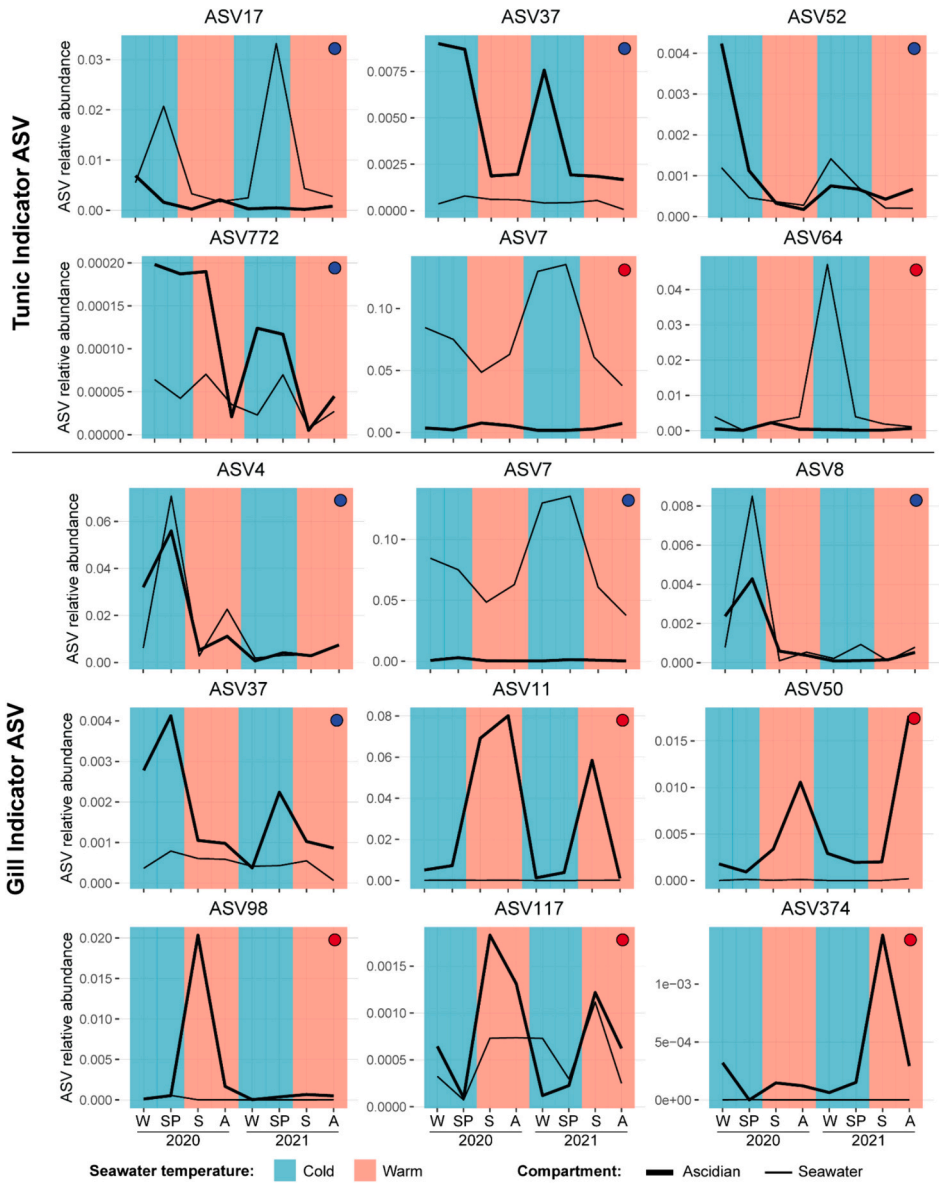

Fig. 4. Seasonal relative abundance trends of indicator ASVs of ascidian tissue samples associated with cold and warm periods and comparison with their relative abundance in seawater samples during the same sampling period. Note that temperature thresholds for cold and warm temperatures are below 17 °C and above 19 °C respectively. W=Winter, SP=Spring, S=Summer, A = Autumn. Blue (Cold) and red (Warm) dots (see web version) in the top-right corner indicate periods to which each ASV is indicator of.

coefficients for both comparisons of ca. 0.8 (Fig. A.4). The localities of Blanes and Vilanova were not significantly different in terms of TE abundance (Table A.9). However, seasonal differences in TE concentrations were found between harbours following a haphazard pattern (Fig. 5b). Our PCA did not show any seasonal pattern in TE concentrations, although a separation between winter and spring 2020 from the other months was evident in both harbours (Fig. 5c).

The RDA combining the microbial composition considering all samples and the temporal trace element values in seawater provided a clear distinction for the two ascidian compartments, with seawater having a central position among samples (Fig. A.5). Since the highest differentiation was related to compartment, we conducted the RDA separately for each one, to associate different microbiome communities with trace elements and identify seasonal trends (Fig. 6). Some general patterns could be detected, albeit with exceptions. The seawater samples showed an ordination along the first axis from cold to warm samples, positively correlating winter communities with the trace elements aluminium, copper, and iron (Fig. 6). Tunic samples displayed no apparent groups in terms of locality or period (Fig. 6). Vilanova samples tended to occupy extreme positive and negative positions along the first axis, with Blanes' samples in a more central position. Finally, the gill RDA showed a general distinction between warm and cold periods, in which cold periods of both localities were positively correlated with zinc, lead, selenium, and copper. On the other hand, for the warm periods, a group of Vilanova samples were positively correlated with iron, whereas other microbiome samples of Blanes and Vilanova were positively correlated with boron (Fig. 6). For seawater community samples, the four first axes of the RDA were significant (Table A.10) with 145 candidate outlier ASVs correlated with TE (Table A.11). For the tunics, only the first axis was found to be significant (Table A.10), with only 10 candidate outlier ASVs correlated (positively and negatively) with TE (Table A.11). Finally, for gills the two first axes were significant (Table A.10), and 19 outlier ASVs were correlated with TE (Table A.11). There were 8 ASVs significantly correlated with TE shared between tunic and gills. Most of them were correlated to different elements with the exception of ASV5 and ASV9, both correlated with lead but

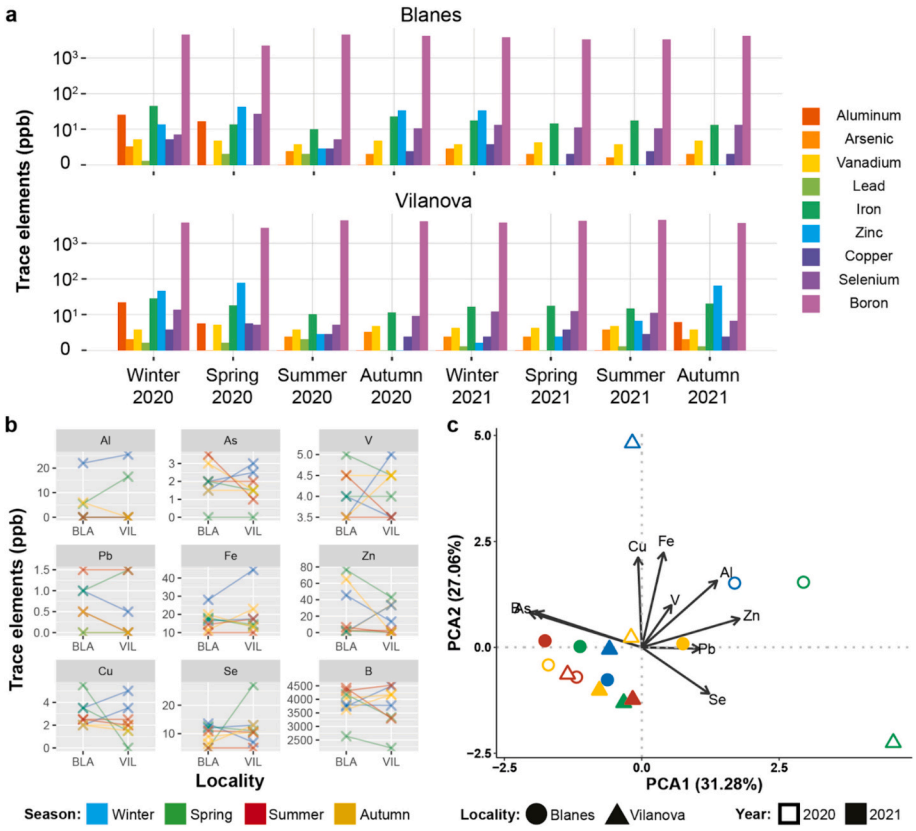

Fig. 5. Trace Element in Blanes (BLA) and Vilanova (VIL) seawater from Winter 2020 to Autumn 2021. **a)** Trace Element concentration (in ppb) during each sampling point in the harbours of Blanes and Vilanova. **b)** Mean trace element concentration for each locality. **c)** PCA organisation of the samples according to their trace element concentration. Al = Aluminium, As = Arsenic, V=Vanadium, Pb = Lead, Fe = Iron, Zn = Zinc, Cu = Copper, Se = Selenium, B=Boron.

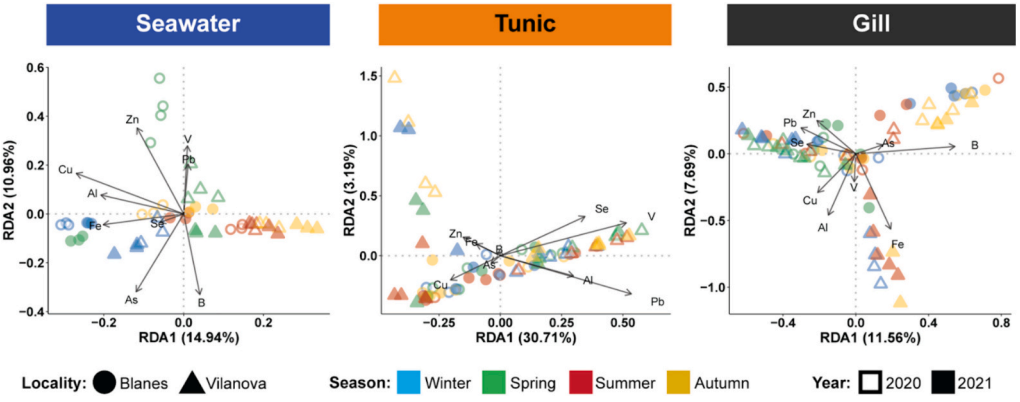

Fig. 6. Redundancy analysis (RDA) of Trace Elements (TE) concentrations and compartment bacterial communities. Note that the constrained variance for seawater was 0.53, for tunic was 0.37, and for gill was 0.27. Al = Aluminium, As = Arsenic, V=Vanadium, Pb = Lead, Fe = Iron, Zn = Zinc, Cu = Copper, Se = Selenium, B=Boron.

positively for gills and negatively for tunics (Table A.11).

4. Discussion

4.1. Seasonal microbial biodiversity

We highlighted an unprecedented bacterial richness in ascidians of >30,000 ASVs, with tunic and gills presenting >15,000 ASVs each. Previous microbiome studies in ascidians claimed that they are host to a rich microbiome but identified lower diversity values (Dror et al., 2019; Evans et al., 2017; López-Legentil et al., 2023; Utermann et al., 2020). However, these studies used OTUs with 97 % identity clustering instead of ASVs, included only a few individuals, generally analysed only tunic samples, and took into consideration a single time-point (with the exception of Dror and collaborators who studied seasonality along a natural year). Recently, ~ 18,500 ASVs of the microbial community of seawater and gill, tunic, and guts of both juvenile and adult stages *of S. plicata* were detected on three different harbours at a single time-point (Galià-Camps et al., 2023). Thus, our 210 samples collected over two years showed an increased microbiome richness and diversity due to the higher number of samples and microbiome shifts over time, likely related to fluctuating environmental conditions. Actually, microbiome shifts have been described in both aquatic and terrestrial species and have been attributed to diet adaptation (Baniel et al., 2021; Lou et al.,

2021), adaptation to anthropogenic pressures (Pass et al., 2015), or a wide combination of multiple factors (Flemer et al., 2022; Palladino et al., 2022). In all of these cases, the number of bacteria was higher than in single snapshot studies.

Bray Curtis dissimilarities in the microbiome community showed a significant interaction of compartment and locality, as already noted in this species at a single time point (Galià-Camps et al., 2023). When analysing the compartments separately, seawater showed a seasonal differentiation, and both locality and period were significant factors that explained a similar amount of variation in microbial community structure. On the other hand, neither gill nor tunic tissues displayed evident seasonal clustering in the MDS configuration. The tunic is composed of a mucopolysaccharide matrix, which acts as an outer cover for *Styela plicata*. This tissue can reach thicknesses of >5 mm in this species. Therefore, considering that we sampled the inner tunic, its associated microbiota might not be so strongly subjected to environmental changes. This fact contrasts with previous studies on *S. plicata* which detected seasonal changes in the tunic's microbial community in Israel and the Atlantic coast of America (Dror et al., 2019). Nevertheless, the inclusion of two years and 5 individuals per season provides a comprehensive picture of the microbiome over time, and we failed to detect seasonal changes over time of the tunic's microbial community. Even if not evident in the MDS, statistical analyses revealed significant differences for periods (warm or cold) in gills. Gills are the filtering organ of ascidians, so they are in tight contact with the surrounding water (Fiala-Médioni, 1978). In addition, gills are highly vascularized structures with intense metabolic activity (Jiang et al., 2023). Their symbiotic bacterial community may be highly influenced by environmental changes, such as temperature and salinity (Galià-Camps et al., 2023; Schreiber et al., 2016). Therefore, gill community shifts likely have an adaptive value in front of temporally changing conditions. Microbiome seasonal shifts have also been reported in vertebrate species such as human gut (Koliada et al., 2020), gelada baboons' gut (Baniel et al., 2021), and fish skin and gut (Escalas et al., 2022; Larsen et al., 2015). Although less explored, seasonal microbiome shifts have also been documented in invertebrates, such as corals (Deignan et al., 2023; Sharp et al., 2017). Interestingly, microbiome seasonal changes have been found to boost the invasive capabilities of introduced fish species in the Mediterranean Sea (Escalas et al., 2022). In this regard, multi-compartment holobionts with complex and rich microbiomes may have an advantage over groups with less structural complexity and diversity as is the case of some low microbial abundance (LMA) sponges (Erwin et al., 2015; Lamb and Watts, 2023; Pita et al., 2013) when it comes to survival in anthropized unstable habitats. Species with several compartments featuring rich and distinct microbiomes, such as *S. plicata*, can draw on existing symbiont diversity and, combined with the horizontal acquisition of bacteria, rapidly adapt their microbiomes (Goddard-Dwyer et al., 2021; Utermann et al., 2020) potentially increasing the holobiont fitness under changing conditions. It can be noted that there is also genetic variability among *S. plicata* populations in the study area as revealed by cytochrome oxidase I allele composition (Pineda et al., 2011). Thus, future studies must try to ascertain the role of population genomic structure in the microbiome composition of this species at several spatial scales, as it is a significant factor in structuring microbiome communities in other ascidian species (Casso et al., 2020).

4.2. Bacterial core temporal patterns

Core bacterial communities are thought to play a crucial part in holobiont survival. However, the composition and relevance of the core community varies across marine holobionts. For instance, both low and high microbial abundance sponges (LMA and HMA, respectively) have a rich core community with relative abundances above 50 % of the bacterial community (Turon et al., 2018). Conversely, coral core communities are highly diverse but are found at low relative abundances (D Ainsworth et al., 2015; Hernandez-Agreda et al., 2018). Ascidian cores comprise a few taxonomic units (either assessed as OTUs or ASVs), with relatively high abundances (Dror et al., 2019; Erwin et al., 2013; Galià-Camps et al., 2023). Interestingly, in our study, no ASV was present in all samples, neither was in all seawater or all ascidian samples separately. This fact is surprising, as previous studies of *S. plicata* claimed that this species has few yet abundant core bacteria (Dror et al., 2019; Erwin et al., 2013; Galià-Camps et al., 2023). The absence of a 100 % core may result from the higher number of samples and the temporal scale of our study. Nevertheless, a less strict 95 % threshold to delineate core communities detected an overall core comprising a single component, ASV76 (*Staphylococcus* sp.). This taxon was not recovered as core in the two previous studies, probably due to its low relative abundance (0.2 % in ascidian samples and 0.03 % in seawater samples). *Staphylococcus* is a bacterial genus found to have beneficial activities such as immune system enhancement and wound healing in model organisms (Brown and Horswill, 2020). The enrichment of *Staphylococcus* ASV76 in the ascidian compared to seawater samples suggests that it may play a role for the host.

When analysing each compartment independently, a rich 95 % core was found for seawater samples (45 ASVs), whereas each ascidian compartment had reduced cores (4 for tunic and 9 for gills, respectively), smaller than previously found in this species (Dror et al., 2019; Erwin et al., 2013; Galià-Camps et al., 2023). We attribute this effect to seasonality, which makes core communities more restricted as the bacteria must persist during cold and warm periods. For the tunic, 3 out of 4 ASVs were coincident with the adult core microbiomes identified in a previous study (Galià-Camps et al., 2023) and for gills there were 8 common ASVs with that previous work, emphasising the relevance of these ASVs for the holobiont survival. Among tunic core bacteria, we can highlight ASV0 (*Methyloceanibacter* sp.), found at high relative abundance. *Methyloceanibacter*, a facultative anaerobic bacteria, is also highly abundant in seawater samples. Therefore, *S. plicata* likely acquire this bacterium from the environment where it could play a role in carbon cycling as found in other environments (Ramírez et al., 2023; Takeuchi et al., 2014). Among the gill core bacteria, ASV1 (Gammaproteobacteria), ASV2, and ASV3 (Indeterminate) are found at high abundances, while ASV5 (*Endozoicomonas* sp.) and ASV6 (Bacteroidales) have low frequencies. Gammaproteobacteria ASV1 and Indeterminate ASV2 are abundant in gills and tunics, although they are infrequent in surrounding seawater samples, suggesting enrichment in the tissues. Gammaproteobacteria ASV1 and Indeterminate ASV2 should be studied in detail in future studies since their abundance and prevalence among samples, and their enrichment in adults vs. juvenile individuals, point to them as potentially relevant bacteria for adaptation, survival, and therefore invasion success of *Styela plicata* (Galià-Camps et al., 2023).

Finally, many ASVs are detected when considering tissue-specific cores separately in warm and cold periods. However, only ASV3 (Indeterminate) for gills during warm periods is highly abundant. The absence of taxonomic assignment for ASV3 hampers the identification of possible functions of this bacterium, but its high abundance points to a possible adaptive role related to warm conditions, extending the host's evolutionary potential. Conversely, other period-specific gill ASVs that appear at lower abundance could be identified at the genus level (*Castellaniella* sp. ASV10, *Parapusillimonas* sp. ASV24, *Stenotrophomonas* sp. ASV31). These bacteria are more abundant during warm periods, coinciding with higher portuary activities linked to leisure boats that spill combustible to the water. Interestingly, *Castellaniella* species (ASV10) have a strong detoxifying and denitrifying potential (Amanze et al., 2023; Spain et al., 2007), whereas *Parapusillomonas* species (ASV24) appear to be powerful crude oil-degrading microbes (Preeti et al., 2015). Thus, although at low abundances, season-specific beneficial core ASVs could be as important as the highly abundant ones, and imbalances in their abundances may result in physiologically altered states of the hosts (Henry et al., 2021). Finally, *Stenotrophomonas* species (ASV31) have beneficial roles in plant interactions by contributing to sulphur and nitrogen cycles and degrading pollutants (An and Berg, 2018). However,

Stenotrophomonas species have also been reported to be opportunistic pathogens that usually infect respiratory systems in a wide variety of organisms, including, among others, deep-sea invertebrates (Brooke, 2012; Ryan et al., 2009). Although we don't know the role played by this bacterium in *S. plicata*, a potential pathogenic role as found in other invertebrates cannot be ruled out. It would not be surprising to see an increase in the prevalence of pathogenic bacteria in warm periods, since high temperatures, in combination with a high abundance of harbour organic material, can negatively affect water quality and potentially contribute to an easier infection of *S. plicata* by pathogens, as also found in other species (Heron et al., 2010; Wang et al., 2021).

4.3. Indicator species highlight strong seasonality

Many ASVs were characterised as indicators for each compartment associated with cold and warm periods. This fact is of prime interest since it indicates that tissue-specific microbiome adaptive shifts for cold and warm periods might be important for the correct functioning of the holobiont and that this potential plasticity is restricted to a few selected bacterial taxa rather than to the whole microbiota. Furthermore, tunic seasonal indicator ASV profiles highlighted two different trends. On the one hand, the abundance of ASV52 (Vibrionaceae) and ASV772 (*Sneathiella* sp.), both bacteria associated with cold periods in tunics, fluctuated in parallel to abundances in seawater, suggesting a quick horizontal transfer of potentially adaptive bacteria. *Sneathiella* species have been reported to degrade polycyclic aromatic hydrocarbons (Sauret et al., 2014), whose proliferation in both environment and tunics might promote the establishment of detoxification pathways. On the other hand, the abundance trends of the other tunic period-associated bacteria are independent of those found in seawater, even opposite in some cases, suggesting that the ascidian tunic might be capable of regulating its symbionts' relative abundances by promoting the proliferation of those specific ASVs that might be seasonally beneficial.

Among indicator ASVs in gills, *Candidatus Hepatoplasma* sp. ASV11 had abundance peaks in the ascidian gill during the warm periods, without parallel abundance trends in seawater samples. This bacterium has been demonstrated to be a beneficial symbiont species in many arthropods, possibly playing a role in nourishment during harsh seasons (Chen et al., 2015; Wang et al., 2004; Zamora-Briseño et al., 2020), and we expand here its symbiotic potential to marine non-arthropod invertebrate species. Similarly, ASV50 (*Endozoicomonas* sp.) showed the same abundance trends as *Candidatus Hepatoplasma* sp. ASV11. Interestingly, *Endozoicomonas* species symbiotic relationships with other marine taxa have been widely reported, in which they play potential roles in carbon sugar transport and utilisation, and in protein secretion (Neave et al., 2017; Pogoreutz et al., 2022). We also found specific gill warm period indicator bacteria ASV98 (Helicobacteraceae), and ASV117 (*Vibrio* sp.) that have been reported as pathogenic and usually infect marine invertebrates (Nakagawa et al., 2017; Neu et al., 2021; Stabili et al., 2012). Furthermore, we found ASV374 (*Flaviflexus* sp.) associated with warm periods and reported to have antimicrobial functions (Nathani et al., 2020). All these gill warm indicator ASVs abundances, except *Vibrio* sp. ASV117, displayed abundances independent from seawater concentrations. Although the functions of these ASVs might be essential throughout the year, their relevance could be increased during warm periods, as high temperatures and high anthropic activity result in stressful conditions for the host (Palladino et al., 2022; Pineda et al., 2012).

Interestingly, the abundance over time of the four cold period indicator ASVs in gill (Cyanobacteriia ASV4, Rhodobacteraceae ASV7, Pirellulaceae ASV8, and Cyanobacteriia ASV37) showed a pattern similar to their abundance in the seawater. This suggests that the host feeds on these species or that the host is capable of obtaining these bacteria by horizontal transmission when abundant in the environment. It is worth noting that Rhodobacteraceae species (ASV7) seem to have beneficial functions against pathogenic elements such as *Vibrio* species (Dong et al., 2021). Similarly, Pirellulaceae species (ASV8) have been reported to synthesise antibacterial compounds (Vitorino et al., 2022). Overall, each tissue seems to host specific bacterial communities that might help them to face pathogenic bacteria and toxic elements, as well as to optimise tissue-specific functions. Only Cyanobacteriia ASV37 is an indicator ASV associated with the cold period of both gill and tunic, indicating its potential importance for the whole organism. Another exception is Rhodobacteraceae ASV7, indicator of tunic during warm periods and indicator for gills during cold periods. Although at very low concentrations, this intercompartmental bacterium could play a dual role in the adaptation and survival of *Styela plicata* over the seasons.

4.4. Environmental and anthropogenic effects shape microbiomes

In a climate change scenario in which human activities shape and modify most natural environments, it is of major relevance to find associations between the adaptive mechanisms of species and environmental conditions (Zenni et al., 2014). Furthermore, as invasive species are about to increase in numbers and extent with globalisation, one key aspect is to investigate how they overcome human-related adverse conditions, a knowledge key to understand evolutionary processes and that may also open options for controlling new colonisation events (Giakoumi et al., 2019; Havel et al., 2015; Roy et al., 2023).

Our study found that the seawater bacterial community and its association with anthropic trace element conditions presented a clear dichotomy between warm and cold periods. Seasonal natural selection operates freely on seawater microbes since they are directly subjected to external environmental factors (Auladell et al., 2022). Conversely, environmental buffering can occur inside ascidian tissues as they shelter the microbial community against toxic trace element shifts (Kiran et al., 2018).

Human pollution is a major disruptor of community organisation at many levels, including changes in the hosts' microbiomes (Palladino et al., 2022; Stock et al., 2021). We detected higher contamination levels of zinc, lead, selenium, aluminium, vanadium, iron, and copper in the spring and winter of 2020, as explained by the first and second axes of the PCA respectively. An episode of exceptional rainfall occurred in the studied area at the beginning of 2020 due to the passage of the Storm Gloria (Sala et al., 2022; Vez-Garzón et al., 2023). Terrestrial runoff increased many-fold, carrying pollutants to the sea, and wastewater treatment plants became saturated. A combination of these factors could increase the harbours' pollutant levels (Parker et al., 2010; Silva et al., 2004). Rainfall and its runoff can affect environmental bacteria (Sala et al., 2022; Vez-Garzón et al., 2023), as well as marine bivalves' microbiomes (Milan et al., 2019). In our case, the tunic microbiome showed no clear association with seawater TE levels. However, gill bacterial communities presented a dichotomy in warm seasons in which some Vilanova samples were associated with iron, whereas a mixture of Vilanova and Blanes' samples was associated with Arsenic. This dichotomy may be indicative of microbiome local adaptation in gills as they are widely exposed to the environment and therefore the effect of anthropogenic changes may impact harder on gill microbiomes. Similar patterns have been described in corals (Kelly et al., 2014; van Oppen et al., 2018), whose polyps have feeding and respiratory functions comparable to those of the ascidian gills.

Gills had more bacteria associated with TE, validating that this tissue is likely more prone to microbiome changes related to external conditions. Nonetheless, in the tunic, some bacteria associated with TE were also found. Interestingly, among the ASVs that could be correlated with TE concentrations, those shared between tunics and gills are those with higher abundance, although mostly associated with different TEs. For instance, Cyanobacteriia ASV4 is an aluminium-associated symbiont in gills, whereas it is vanadium-associated in tunics. The abundance of this ASV in gills mirrors that in the surrounding seawater, pointing to a potential acquisition from the environment. Among tissue-specific bacteria associated with TE, we identified at the genus level *Candidatus*

Hepatoplasma sp. ASV11, *Pseudomonas* sp. ASV13, *Streptococcus* sp. ASV22, *Acinetobacter* sp. ASV25, *Endozoicomonas* sp. ASV50 and *Gracilibacteria* sp. ASV51 on gills, and *Castellaniella* sp. ASV10 and *Pseudomonas* sp. ASV108 in tunics. The presence of *Acinetobacter* species, whose members have been repeatedly reported to be pathogens, could possibly represent infections of the host during immunosuppression periods driven by high abundance of TEs (Manchanda et al., 2010), while species of the genus *Gracilibacteri*a seem to contribute to sulphur cycling on deep-sea anemones (Goffredi et al., 2021). Overall, these ASVs likely contribute to the adaptation process in these two chemically and environmentally different harbours.

5. Conclusions

The present study has revealed a clear differentiation between seawater bacterial communities and the tissues of *Styela plicata*, with both gills and tunic microbiomes composed of distinct communities defined by a few core bacteria thought to have a potentially high adaptive value. Furthermore, seasonal patterns at the microbial community level have been unveiled, especially in seawater samples, followed by gills, and being almost absent in tunic samples. Interestingly, significant differences have also been found between localities separated by only ~ 100 km, likely reflecting that the different sizes and activity levels (fishing, leisure, commercial) of the harbours studied can be reflected in differences in the microbiome of local *S. plicata* individuals. These results imply that fine-scale studies on invasive holobionts should consider compartment-specific spatio-temporal trends since different underlying dynamics can exist, and generalisation becomes difficult. Failure to perform low-level taxonomic assignments for many ASVs due to gaps in the reference databases has hampered the identification of the possible roles of some bacteria. This fact highlights the need to complete the reference databases to fully characterise symbiont microbial diversity. Nevertheless, we have identified specific bacteria related to cold and warm periods with pathogenic, metabolic, and antibacterial activities. We point out that seasonal adaptation and pathogen-antibiotic interplay are necessary processes for invasive success that likely rely on a few key bacterial species. Lastly, many ASVs are correlated with trace element concentrations, most likely driven by human activities. We encourage future studies to explore anthropogenic conditions other than trace elements to fully disentangle the potential of the adaptive role of bacteria in the holobiont fitness. We conclude that the microbial communities of *S. plicata* change as a response to environmental changes and harmful elements. This plasticity can turn this species into a well-adapted holobiont in highly anthropized areas, which may explain why it is one of the most successful invasive species worldwide.

Supplementary data to this article can be found online at https://doi.org/10.1016/j.marpolbul.2024.116477.

CRediT authorship contribution statement

Carles Galià-Camps: Writing – review & editing, Writing – original draft, Visualization, Software, Resources, Methodology, Investigation, Formal analysis, Data curation, Conceptualization. **Liam Junkin:** Visualization, Resources, Investigation, Formal analysis, Data curation. **Xavier Borrallo:** Resources, Investigation, Data curation. **Carlos Carreras:** Writing – review & editing, Validation, Supervision, Software, Resources, Project administration, Methodology, Funding acquisition, Conceptualization. **Marta Pascual:** Writing – review & editing, Validation, Supervision, Resources, Project administration, Methodology, Funding acquisition, Conceptualization. **Xavier Turon:** Writing – review & editing, Validation, Supervision, Software, Resources, Project administration, Methodology, Funding acquisition, Conceptualization.

Declaration of competing interest

The authors declare that they have no known competing financial interests or personal relationships that could have appeared to influence the work reported in this paper.

Data availability

Raw reads generated in the present study are deposited in NCBI with the bioproject code: PRJNA1030313. BioSamples SAMN37904220–SAMN37904357 correspond to the host's tissue microbiomes, and BioSamples SAMN37904613–SAMN37904654 correspond to seawater microbiomes. Processed read abundance tables can be found in Table A.3. Environmental variables (Temperature, Salinity, and Trace Element concentrations), can be found in Table A.8. R scripts used for this study are uploaded to https://github.com/CGaliaCamps/spatio-temporal_microbiome.

Acknowledgements

The authors want to thank Elena Baños, Oriol Castells, Gisela Marín, Astrid Luna, Adrià Antich, Jesús Zarcero, and Laia Romano for their assistance during samplings. Also, to the Port authorities of the harbours of Vilanova and Blanes for granting access to their facilities for sampling. Finally we want to thank Robert Benaiges, who aided us to update taxonomic nomenclature with the new prokaryote code.

Funding sources

This work was supported by the Spanish Ministry of Science and Innovation [grant number PID2020-118550RB - MICIU/AEI/10.13039/501100011033], and the Agency for Management of University and Research Grants (AGAUR) [2021 SGR 00405, 2021 SGR 01271]. CG was granted by the Spanish Ministry of Science, Innovations and Universities and European Social Funds [grant number PRE-2018-085227 - MICIU/AEI/10.13039501100011033].

References

Aldred, N., Clare, A.S., 2014. Mini-review: impact and dynamics of surface fouling by solitary and compound ascidians. Biofouling 30, 259–270. https://doi.org/10.1080/08927014.2013.866653.

Amanze, C., Anaman, R., Wu, X., Alhassan, S.I., Yang, K., Fosua, B.A., Yunhui, T., Yu, R., Wu, X., Shen, L., Dolgor, E., Zeng, W., 2023. Heterotrophic anodic denitrification coupled with cathodic metals recovery from on-site smelting wastewater with a bioelectrochemical system inoculated with mixed *Castellaniella* species. Water Res. 231, 119655 https://doi.org/10.1016/j.watres.2023.119655.

An, S.-Q., Berg, G., 2018. Stenotrophomonas maltophilia. Trends Microbiol. 26, 637–638. https://doi.org/10.1016/j.tim.2018.04.006.

Antich, A., Palacin, C., Wangensteen, O.S., Turon, X., 2021. To denoise or to cluster, that is not the question: optimizing pipelines for COI metabarcoding and metaphylogeography. BMC Bioinform. 22, 177. https://doi.org/10.1186/s12859-021-04115-6.

Auladell, A., Barberán, A., Logares, R., Garcés, E., Gasol, J.M., Ferrera, I., 2022. Seasonal niche differentiation among closely related marine bacteria. ISME J. 16, 178–189. https://doi.org/10.1038/s41396-021-01053-2.

Baedke, J., Fábregas-Tejeda, A., Nieves Delgado, A., 2020. The holobiont concept before Margulis. J. Exp. Zool. B Mol. Dev. Evol. 334, 149–155. https://doi.org/10.1002/jez.b.22931.

Baniel, A., Amato, K.R., Beehner, J.C., Bergman, T.J., Mercer, A., Perlman, R.F., Petrullo, L., Reitsema, L., Sams, S., Lu, A., Snyder-Mackler, N., 2021. Seasonal shifts in the gut microbiome indicate plastic responses to diet in wild geladas. Microbiome 9, 26. https://doi.org/10.1186/s40168-020-00977-9.

Borden, J.B., Flory, S.L., 2021. Urban evolution of invasive species. Front. Ecol. Environ. 19, 184–191. https://doi.org/10.1002/fee.2295.

Breusch, T.S., Pagan, A.R., 1979. A simple test for heteroscedasticity and random coefficient variation. Econometrica 47, 1287–1294. https://doi.org/10.2307/1911963.

Brooke, J.S., 2012. *Stenotrophomonas maltophilia*: an emerging global opportunistic pathogen. Clin. Microbiol. Rev. 25, 2–41. https://doi.org/10.1128/CMR.00019-11.

Brown, M.M., Horswill, A.R., 2020. *Staphylococcus epidermidis*-skin friend or foe? PLoS Pathog. 16, e1009026 https://doi.org/10.1371/journal.ppat.1009026.

Callahan, B.J., McMurdie, P.J., Rosen, M.J., Han, A.W., Johnson, A.J.A., Holmes, S.P., 2016. DADA2: high-resolution sample inference from Illumina amplicon data. Nat. Methods 13, 581–583. https://doi.org/10.1038/nmeth.3869.

Caporaso, J.G., Lauber, C.L., Walters, W.A., Berg-Lyons, D., Lozupone, C.A., Turnbaugh, P.J., Fierer, N., Knight, R., 2011. Global patterns of 16S rRNA diversity

at a depth of millions of sequences per sample. Proc. Natl. Acad. Sci. U. S. A. 108 (Suppl. 1), 4516–4522. https://doi.org/10.1073/pnas.1000080107.
Casso, M., Turon, M., Marco, N., Pascual, M., Turon, X., 2020. The microbiome of the worldwide invasive ascidian *Didemnum vexillum*. Front. Mar. Sci. 7 https://doi.org/10.3389/fmars.2020.00201.
Chen, H., Boutros, P.C., 2011. VennDiagram: a package for the generation of highly-customizable Venn and Euler diagrams in R. BMC Bioinform. 12, 35. https://doi.org/10.1186/1471-2105-12-35.
Chen, X., Di, P., Wang, H., Li, B., Pan, Y., Yan, S., Wang, Y., 2015. Bacterial community associated with the intestinal tract of Chinese mitten crab (*Eriocheir sinensis*) farmed in Lake Tai, China. PLoS One 10, e0123990. https://doi.org/10.1371/journal.pone.0123990.
Chen, Y., Liu, Q., Xu, M., Wang, Z., 2020. Inter-annual variability of heavy metals pollution in surface sediments of Jiangsu coastal region, China: case study of the Dafeng Port. Mar. Pollut. Bull. 150, 110720 https://doi.org/10.1016/j.marpolbul.2019.110720.
Cheng, C., Wickham, J.D., Chen, L., Xu, D., Lu, M., Sun, J., 2018. Bacterial microbiota protect an invasive bark beetle from a pine defensive compound. Microbiome 6, 132. https://doi.org/10.1186/s40168-018-0518-0.
Connelly, N.A., O'Neill Jr., C.R., Knuth, B.A., Brown, T.L., 2007. Economic impacts of zebra mussels on drinking water treatment and electric power generation facilities. Environ. Manag. 40, 105–112. https://doi.org/10.1007/s00267-006-0296-5.
Conway, J.R., Lex, A., Gehlenborg, N., 2017. UpSetR: an R package for the visualization of intersecting sets and their properties. Bioinformatics 33, 2938–2940. https://doi.org/10.1093/bioinformatics/btx364.
D Ainsworth, T., Krause, L., Bridge, T., Torda, G., Raina, J.-B., Zakrzewski, M., Gates, R. D., Padilla-Gamiño, J.L., Spalding, H.L., Smith, C., Woolsey, E.S., Bourne, D.G., Bongaerts, P., Hoegh-Guldberg, O., Leggat, W., 2015. The coral core microbiome identifies rare bacterial taxa as ubiquitous endosymbionts. ISME J. 9, 2261–2274. https://doi.org/10.1038/ismej.2015.39.
De Cáceres, M., Legendre, P., 2009. Associations between species and groups of sites: indices and statistical inference. Ecology 90, 3566–3574. https://doi.org/10.1890/08-1823.1.
Dearing, M.D., Kaltenpoth, M., Gershenzon, J., 2022. Demonstrating the role of symbionts in mediating detoxification in herbivores. Symbiosis 87, 59–66. https://doi.org/10.1007/s13199-022-00863-y.
Deignan, L.K., Pwa, K.H., Loh, A.A.R., Rice, S.A., McDougald, D., 2023. The microbiomes of two Singaporean corals show site-specific differentiation and variability that correlates with the seasonal monsoons. Coral Reefs 42, 677–691. https://doi.org/10.1007/s00338-023-02376-6.
Dong, P., Guo, H., Wang, Y., Wang, R., Chen, H., Zhao, Y., Wang, K., Zhang, D., 2021. Gastrointestinal microbiota imbalance is triggered by the enrichment of *Vibrio* in subadult *Litopenaeus vannamei* with acute hepatopancreatic necrosis disease. Aquaculture 533, 736199. https://doi.org/10.1016/j.aquaculture.2020.736199.
Dragičević, P., Bielen, A., Petrić, I., Vuk, M., Žučko, J., Hudina, S., 2021. Microbiome of the successful freshwater invader, the signal crayfish, and its changes along the invasion range. Microbiol. Spectr. 9, e0038921 https://doi.org/10.1128/Spectrum.00389-21.
Dror, H., Novak, L., Evans, J.S., López-Legentil, S., Shenkar, N., 2019. Core and dynamic microbial communities of two invasive ascidians: can host-symbiont dynamics plasticity affect invasion capacity? Microb. Ecol. 78, 170–184. https://doi.org/10.1007/s00248-018-1276-z.
Edgar, R.C., Haas, B.J., Clemente, J.C., Quince, C., Knight, R., 2011. UCHIME improves sensitivity and speed of chimera detection. Bioinformatics 27, 2194–2200. https://doi.org/10.1093/bioinformatics/btr381.
Erwin, P.M., Carmen Pineda, M., Webster, N., Turon, X., López-Legentil, S., 2013. Small core communities and high variability in bacteria associated with the introduced ascidian *Styela plicata*. Symbiosis 59, 35–46. https://doi.org/10.1007/s13199-012-0204-0.
Erwin, P.M., Coma, R., López-Sendino, P., Serrano, E., Ribes, M., 2015. Stable symbionts across the HMA-LMA dichotomy: low seasonal and interannual variation in sponge-associated bacteria from taxonomically diverse hosts. FEMS Microbiol. Ecol. 91 https://doi.org/10.1093/femsec/fiv115.
Escalas, A., Auguet, J.-C., Avouac, A., Belmaker, J., Dailianis, T., Kiflawi, M., Pickholtz, R., Skouradakis, G., Villéger, S., 2022. Shift and homogenization of gut microbiome during invasion in marine fishes. Anim. Microbiome 4, 37. https://doi.org/10.1186/s42523-022-00181-0.
Evans, J.S., Erwin, P.M., Shenkar, N., López-Legentil, S., 2017. Introduced ascidians harbor highly diverse and host-specific symbiotic microbial assemblages. Sci. Rep. 7, 11033 https://doi.org/10.1038/s41598-017-11441-4.
Ferrario, J., Caronni, S., Occhipinti-Ambrogi, A., Marchini, A., 2017. Role of commercial harbours and recreational marinas in the spread of non-indigenous fouling species. Biofouling 33, 651–660. https://doi.org/10.1080/08927014.2017.1351958.
Fiala-Médioni, A., 1978. Filter-feeding ethology of benthic invertebrates (ascidians). IV. Pumping rate, filtration rate, filtration efficiency. Mar. Biol. 48, 243–249. https://doi.org/10.1007/bf00397151.
Flemer, B., Gulati, S., Bergna, A., Rändler, M., Cernava, T., Witzel, K., Berg, G., Grosch, R., 2022. Biotic and abiotic stress factors induce microbiome shifts and enrichment of distinct beneficial bacteria in tomato roots. Phytobiomes J. 6, 276–289. https://doi.org/10.1094/pbiomes-10-21-0067-r.
Galià-Camps, C., Baños, E., Pascual, M., Carreras, C., Turon, X., 2023. Multidimensional variability of the microbiome of an invasive ascidian species. iScience, 107812. https://doi.org/10.1016/j.isci.2023.107812.
Galià-Camps, C., Schell, T., Pegueroles, C., Baranski, D., Hamadou, A.B., Turon, X., Pascual, M., Greve, C., Carreras, C., 2024. Genomic richness enables worldwide invasive success. Res. Sq. https://doi.org/10.21203/rs.3.rs-3902873/v1.
Giakoumi, S., Katsanevakis, S., Albano, P.G., Azzurro, E., Cardoso, A.C., Cebrian, E., Deidun, A., Edelist, D., Francour, P., Jimenez, C., Mačić, V., Occhipinti-Ambrogi, A., Rilov, G., Sghaier, Y.R., 2019. Management priorities for marine invasive species. Sci. Total Environ. 688, 976–982. https://doi.org/10.1016/j.scitotenv.2019.06.282.
Goddard-Dwyer, M., López-Legentil, S., Erwin, P.M., 2021. Microbiome variability across the native and invasive ranges of the ascidian *Clavelina oblonga*. Appl. Environ. Microbiol. 87 https://doi.org/10.1128/AEM.02233-20.
Goffredi, S.K., Motooka, C., Fike, D.A., Gusmão, L.C., Tilic, E., Rouse, G.W., Rodríguez, E., 2021. Mixotrophic chemosynthesis in a deep-sea anemone from hydrothermal vents in the Pescadero Basin, Gulf of California. BMC Biol. 19, 8. https://doi.org/10.1186/s12915-020-00921-1.
Graffelman, J., van Eeuwijk, F., 2005. Calibration of multivariate scatter plots for exploratory analysis of relations within and between sets of variables in genomic research. Biom. J. 47, 863–879. https://doi.org/10.1002/bimj.200510177.
Gu, Z., Gu, L., Eils, R., Schlesner, M., Brors, B., 2014. Circlize implements and enhances circular visualization in R. Bioinformatics 30, 2811–2812. https://doi.org/10.1093/bioinformatics/btu393.
Hall, M., Beiko, R.G., 2018. 16S rRNA gene analysis with QIIME2. Methods Mol. Biol. 1849, 113–129. https://doi.org/10.1007/978-1-4939-8728-3_8.
Han, L., Hao, P., Wang, W., Wu, Y., Ruan, S., Gao, C., Tian, W., Tian, Y., Li, X., Wang, L., Zhang, W., Wang, H., Chang, Y., Ding, J., 2023. Molecular mechanisms that regulate the heat stress response in sea urchins (*Strongylocentrotus intermedius*) by comparative heat tolerance performance and whole-transcriptome RNA sequencing. Sci. Total Environ. 901, 165846 https://doi.org/10.1016/j.scitotenv.2023.165846.
Havel, J.E., Kovalenko, K.E., Thomaz, S.M., Amalfitano, S., Kats, L.B., 2015. Aquatic invasive species: challenges for the future. Hydrobiologia 750, 147–170. https://doi.org/10.1007/s10750-014-2166-0.
Henry, L.P., Bruijning, M., Forsberg, S.K.G., Ayroles, J.F., 2021. The microbiome extends host evolutionary potential. Nat. Commun. 12, 5141. https://doi.org/10.1038/s41467-021-25315-x.
Hernandez-Agreda, A., Leggat, W., Bongaerts, P., Herrera, C., Ainsworth, T.D., 2018. Rethinking the coral microbiome: simplicity exists within a diverse microbial biosphere. MBio 9. https://doi.org/10.1128/mBio.00812-18.
Heron, S.F., Willis, B.L., Skirving, W.J., Eakin, C.M., Page, C.A., Miller, I.R., 2010. Summer hot snaps and winter conditions: modelling white syndrome outbreaks on great barrier reef corals. PloS One 5, e12210. https://doi.org/10.1371/journal.pone.0012210.
Jiang, A., Zhang, W., Wei, J., Liu, P., Dong, B., 2023. Transcriptional analysis of the Endostyle reveals pharyngeal organ functions in ascidian. Biology 12. https://doi.org/10.3390/biology12020245.
Kelly, L.W., Williams, G.J., Barott, K.L., Carlson, C.A., Dinsdale, E.A., Edwards, R.A., Haas, A.F., Haynes, M., Lim, Y.W., McDole, T., Nelson, C.E., Sala, E., Sandin, S.A., Smith, J.E., Vermeij, M.J.A., Youle, M., Rohwer, F., 2014. Local genomic adaptation of coral reef-associated microbiomes to gradients of natural variability and anthropogenic stressors. Proc. Natl. Acad. Sci. U. S. A. 111, 10227–10232. https://doi.org/10.1073/pnas.1403319111.
Kiran, G.S., Sekar, S., Ramasamy, P., Thinesh, T., Hassan, S., Lipton, A.N., Ninawe, A.S., Selvin, J., 2018. Marine sponge microbial association: towards disclosing unique symbiotic interactions. Mar. Environ. Res. 140, 169–179. https://doi.org/10.1016/j.marenvres.2018.04.017.
Koliada, A., Moseiko, V., Romanenko, M., Piven, L., Lushchak, O., Kryzhanovska, N., Guryanov, V., Vaiserman, A., 2020. Seasonal variation in gut microbiota composition: cross-sectional evidence from Ukrainian population. BMC Microbiol. 20, 100 https://doi.org/10.1186/s12866-020-01786-8.
Koskella, B., Hall, L.J., Metcalf, C.J.E., 2017. The microbiome beyond the horizon of ecological and evolutionary theory. Nat. Ecol. Evol. 1, 1606–1615. https://doi.org/10.1038/s41559-017-0340-2.
Lahti, L., Shetty, S., 2012-2019. Tools for microbiome analysis in R. Microbiome package.
Lamb, C.E., Watts, J.E.M., 2023. Microbiome species diversity and seasonal stability of two temperate marine sponges *Hymeniacidon perlevis* and *Suberites massa*. Environ. Microbiome 18, 52. https://doi.org/10.1186/s40793-023-00508-7.
Larsen, A.M., Bullard, S.A., Womble, M., Arias, C.R., 2015. Community structure of skin microbiome of Gulf killifish, *Fundulus grandis*, is driven by seasonality and not exposure to oiled sediments in a Louisiana salt marsh. Microb. Ecol. 70, 534–544. https://doi.org/10.1007/s00248-015-0578-7.
Lenth, R., Singmann, H., Love, J., Buerkner, P., Herve, M., 2020. Emmeans: estimated marginal means. R package version 1.4. 4. Am. Stat.
Lindsay, E.C., Metcalfe, N.B., Llewellyn, M.S., 2020. The potential role of the gut microbiota in shaping host energetics and metabolic rate. J. Anim. Ecol. 89, 2415–2426. https://doi.org/10.1111/1365-2656.13327.
López-Legentil, S., Legentil, M.L., Erwin, P.M., Turon, X., 2015. Harbor networks as introduction gateways: contrasting distribution patterns of native and introduced ascidians. Biol. Invasions 17, 1623–1638. https://doi.org/10.1007/s10530-014-0821-z.
López-Legentil, S., Palanisamy, S.K., Smith, K.F., McCormack, G., Erwin, P.M., 2023. Prokaryotic symbiont communities in three ascidian species introduced in both Ireland and New Zealand. Environ. Sci. Pollut. Res. Int. 30, 6805–6817. https://doi.org/10.1007/s11356-022-22652-2.
Lou, Y., Li, Y., Lu, B., Liu, Q., Yang, S.-S., Liu, B., Ren, N., Wu, W.-M., Xing, D., 2021. Response of the yellow mealworm (*Tenebrio molitor*) gut microbiome to diet shifts during polystyrene and polyethylene biodegradation. J. Hazard. Mater. 416, 126222 https://doi.org/10.1016/j.jhazmat.2021.126222.
Magoč, T., Salzberg, S.L., 2011. FLASH: fast length adjustment of short reads to improve genome assemblies. Bioinformatics 27, 2957–2963. https://doi.org/10.1093/bioinformatics/btr507.

Manchanda, V., Sanchaita, S., Singh, N., 2010. Multidrug resistant acinetobacter. J. Glob. Infect. Dis. 2, 291–304. https://doi.org/10.4103/0974-777X.68538.
Martinez Arbizu, P., 2020. PairwiseAdonis: Pairwise multilevel comparison using adonis. R package version 0.4, 1.
Milan, M., Smits, M., Dalla Rovere, G., Iori, S., Zampieri, A., Carraro, L., Martino, C., Papetti, C., Ianni, A., Ferri, N., Iannaccone, M., Patarnello, T., Brunetta, R., Ciofi, C., Grotta, L., Arcangeli, G., Bargelloni, L., Cardazzo, B., Martino, G., 2019. Host-microbiota interactions shed light on mortality events in the striped venus clam *Chamelea gallina*. Mol. Ecol. 28, 4486–4499. https://doi.org/10.1111/mec.15227.
Nakagawa, S., Saito, H., Tame, A., Hirai, M., Yamaguchi, H., Sunata, T., Aida, M., Muto, H., Sawayama, S., Takaki, Y., 2017. Microbiota in the coelomic fluid of two common coastal starfish species and characterization of an abundant Helicobacter-related taxon. Sci. Rep. 7, 8764. https://doi.org/10.1038/s41598-017-09355-2.
Nathani, N.M., Mootapally, C., Gadhvi, I.R., Maitreya, B., Joshi, C.G. (Eds.), 2020. Marine niche: applications in pharmaceutical sciences: translational research, 1st ed. Springer, Singapore, Singapore. https://doi.org/10.1007/978-981-15-5017-1.
Neave, M.J., Michell, C.T., Apprill, A., Voolstra, C.R., 2017. *Endozoicomonas* genomes reveal functional adaptation and plasticity in bacterial strains symbiotically associated with diverse marine hosts. Sci. Rep. 7, 40579 https://doi.org/10.1038/srep40579.
Neu, A.T., Hughes, I.V., Allen, E.E., Roy, K., 2021. Decade-scale stability and change in a marine bivalve microbiome. Mol. Ecol. 30, 1237–1250. https://doi.org/10.1111/mec.15796.
Nikolaou, A., Tsirintanis, K., Rilov, G., Katsanevakis, S., 2023. Invasive fish and sea urchins drive the status of canopy forming macroalgae in the Eastern Mediterranean. Biology 12. https://doi.org/10.3390/biology12060763.
Oksanen, J., Blanchet, F.G., Kindt, R., Legendre, P., Minchin, P.R., O'Hara, R.B., Simpson, G.L., Solymos, P., Stevens, M.H.H., Wagner, H., Others, 2013. Package "vegan.". In: Community ecology package, version 2, pp. 1–295.
van Oppen, M.J.H., Bongaerts, P., Frade, P., Peplow, L.M., Boyd, S.E., Nim, H.T., Bay, L. K., 2018. Adaptation to reef habitats through selection on the coral animal and its associated microbiome. Mol. Ecol. 27, 2956–2971. https://doi.org/10.1111/mec.14763.
Oren, A., Arahal, D.R., Göker, M., Moore, E.R.B., Rossello-Mora, R., Sutcliffe, I.C., 2023. International Code of Nomenclature of Prokaryotes. Prokaryotic Code (2022 Revision). Int. J. Syst. Evol. Microbiol. 73 https://doi.org/10.1099/ijsem.0.005585.
Palladino, G., Rampelli, S., Galià-Camps, C., Scicchitano, D., Trapella, G., Nanetti, E., Angelini, V., Cleo, D., Turroni, S., Corinaldesi, C., Candela, M., 2022. Plasticity of the *Anemonia viridis* microbiota in response to different levels of combined anthropogenic and environmental stresses. Front. Mar. Sci. 9 https://doi.org/10.3389/fmars.2022.956899.
Parker, J.K., McIntyre, D., Noble, R.T., 2010. Characterizing fecal contamination in stormwater runoff in coastal North Carolina, USA. Water Res. 44, 4186–4194. https://doi.org/10.1016/j.watres.2010.05.018.
Pass, D.A., Morgan, A.J., Read, D.S., Field, D., Weightman, A.J., Kille, P., 2015. The effect of anthropogenic arsenic contamination on the earthworm microbiome. Environ. Microbiol. 17, 1884–1896. https://doi.org/10.1111/1462-2920.12712.
Pineda, M.C., López-Legentil, S., Turon, X., 2011. The whereabouts of an ancient wanderer: global phylogeography of the solitary ascidian *Styela plicata*. PloS One 6, e25495. https://doi.org/10.1371/journal.pone.0025495.
Pineda, M.C., Turon, X., López-Legentil, S., 2012. Stress levels over time in the introduced ascidian *Styela plicata*: the effects of temperature and salinity variations on hsp70 gene expression. Cell Stress Chaperones 17, 435–444. https://doi.org/10.1007/s12192-012-0321-y.
Pita, L., Turon, X., López-Legentil, S., Erwin, P.M., 2013. Host rules: spatial stability of bacterial communities associated with marine sponges (*Ircinia* spp.) in the Western Mediterranean Sea. FEMS Microbiol. Ecol. 86, 268–276. https://doi.org/10.1111/1574-6941.12159.
Pogoreutz, C., Oakley, C.A., Rädecker, N., Cárdenas, A., Perna, G., Xiang, N., Peng, L., Davy, S.K., Ngugi, D.K., Voolstra, C.R., 2022. Coral holobiont cues prime *Endozoicomonas* for a symbiotic lifestyle. ISME J. 16, 1883–1895. https://doi.org/10.1038/s41396-022-01226-7.
Preeti, S., Parmar, D., Pandya, A., 2015. Comparative study of crude oil degradation efficiency of microbes isolated from crude oil contaminated site. Bull. Env. Pharmacol. Life Sci. 4, 91–94.
Quast, C., Pruesse, E., Yilmaz, P., Gerken, J., Schweer, T., Yarza, P., Peplies, J., Glöckner, F.O., 2013. The SILVA ribosomal RNA gene database project: improved data processing and web-based tools. Nucleic Acids Res. 41, D590–D596. https://doi.org/10.1093/nar/gks1219.
Ramírez, G.A., Bar-Shalom, R., Furlan, A., Romeo, R., Gavagnin, M., Calabrese, G., Garber, A.I., Steindler, L., 2023. Bacterial aerobic methane cycling by the marine sponge-associated microbiome. Microbiome 11, 49. https://doi.org/10.1186/s40168-023-01467-4.
Revelle, W., 2015. Package "psych".
Rizvi, A., Ahmed, B., Saghir Khan, M., Rajput, V.D., Umar, S., Minkina, T., Lee, J., 2022. Maize associated bacterial microbiome linked mitigation of heavy metal stress: a multidimensional detoxification approach. Environ. Exp. Bot. 200, 104911 https://doi.org/10.1016/j.envexpbot.2022.104911.
Rodríguez-Martínez, R.E., Medina-Valmaseda, A.E., Blanchon, P., Monroy-Velázquez, L. V., Almazán-Becerril, A., Delgado-Pech, B., Vásquez-Yeomans, L., Francisco, V., García-Rivas, M.C., 2019. Faunal mortality associated with massive beaching and decomposition of pelagic *Sargassum*. Mar. Pollut. Bull. 146, 201–205. https://doi.org/10.1016/j.marpolbul.2019.06.015.
Rosenberg, E., Zilber-Rosenberg, I., 2018. The hologenome concept of evolution after 10 years. Microbiome 6, 78. https://doi.org/10.1186/s40168-018-0457-9.
Roy, H.E., Pauchard, A., Stoett, P., Renard Truong, T., Bacher, S., Galil, B.S., Hulme, P.E., Ikeda, T., Sankaran, K.V., McGeoch, M.A., Meyerson, L.A., Nuñez, M.A., Ordonez, A., Rahlao, S.J., Schwindt, E., Seebens, H., Sheppard, A.W., Vandvik, V., 2023. IPBES Invasive Alien Species assessment: Summary for Policymakers. https://doi.org/10.5281/ZENODO.7430692.
Ryan, R.P., Monchy, S., Cardinale, M., Taghavi, S., Crossman, L., Avison, M.B., Berg, G., van der Lelie, D., Dow, J.M., 2009. The versatility and adaptation of bacteria from the genus *Stenotrophomonas*. Nat. Rev. Microbiol. 7, 514–525. https://doi.org/10.1038/nrmicro2163.
Sala, M.M., Peters, F., Sebastián, M., Cardelús, C., Calvo, E., Marrasé, C., Massana, R., Pelejero, C., Sala-Coromina, J., Vaqué, D., Gasol, J.M., 2022. COVID-19 lockdown moderately increased oligotrophy at a marine coastal site. Sci. Total Environ. 812, 151443 https://doi.org/10.1016/j.scitotenv.2021.151443.
Sauret, C., Séverin, T., Vétion, G., Guigue, C., Goutx, M., Pujo-Pay, M., Conan, P., Fagervold, S.K., Ghiglione, J.-F., 2014. "Rare biosphere" bacteria as key phenanthrene degraders in coastal seawaters. Environ. Pollut. 194, 246–253. https://doi.org/10.1016/j.envpol.2014.07.024.
Schrader, L., Kim, J.W., Ence, D., Zimin, A., Klein, A., Wyschetzki, K., Weichselgartner, T., Kemena, C., Stökl, J., Schultner, E., Wurm, Y., Smith, C.D., Yandell, M., Heinze, J., Gadau, J., Oettler, J., 2014. Transposable element islands facilitate adaptation to novel environments in an invasive species. Nat. Commun. 5, 5495 https://doi.org/10.1038/ncomms6495.
Schreiber, L., Kjeldsen, K.U., Funch, P., Jensen, J., Obst, M., López-Legentil, S., Schramm, A., 2016. *Endozoicomonas* are specific, facultative symbionts of sea squirts. Front. Microbiol. 7, 1042. https://doi.org/10.3389/fmicb.2016.01042.
Sharp, K.H., Pratte, Z.A., Kerwin, A.H., Rotjan, R.D., Stewart, F.J., 2017. Season, but not symbiont state, drives microbiome structure in the temperate coral *Astrangia poculata*. Microbiome 5, 120. https://doi.org/10.1186/s40168-017-0329-8.
Silva, S., Ré, A., Pestana, P., Rodrigues, A., Quintino, V., 2004. Sediment disturbance off the Tagus estuary, Western Portugal: chronic contamination, sewage outfall operation and runoff events. Mar. Pollut. Bull. 49, 154–162. https://doi.org/10.1016/j.marpolbul.2004.02.004.
Singh, B.K., Liu, H., Trivedi, P., 2020. Eco-holobiont: a new concept to identify drivers of host-associated microorganisms. Environ. Microbiol. 22, 564–567. https://doi.org/10.1111/1462-2920.14900.
Sodhi, N.S., Ehrlich, P.R., 2010. Conservation Biology for All. Oxford University Press.
Spain, A.M., Peacock, A.D., Istok, J.D., Elshahed, M.S., Najar, F.Z., Roe, B.A., White, D.C., Krumholz, L.R., 2007. Identification and isolation of a *Castellaniella* species important during biostimulation of an acidic nitrate- and uranium-contaminated aquifer. Appl. Environ. Microbiol. 73, 4892–4904. https://doi.org/10.1128/AEM.00331-07.
Stabili, L., Cardone, F., Alifano, P., Tredici, S.M., Piraino, S., Corriero, G., Gaino, E., 2012. Epidemic mortality of the sponge *Ircinia variabilis* (Schmidt, 1862) associated to proliferation of a *Vibrio* bacterium. Microb. Ecol. 64, 802–813. https://doi.org/10.1007/s00248-012-0068-0.
Stern, D.B., Lee, C.E., 2020. Evolutionary origins of genomic adaptations in an invasive copepod. Nat. Ecol. Evol. 4, 1084–1094. https://doi.org/10.1038/s41559-020-1201-y.
Stock, W., Callens, M., Houwenhuyse, S., Schols, R., Goel, N., Coone, M., Theys, C., Delnat, V., Boudry, A., Eckert, E.M., Laspoumaderes, C., Grossart, H.P., De Meester, L., Stoks, R., Sabbe, K., Decaestecker, E., 2021. Human impact on symbioses between aquatic organisms and microbes. Aquat. Microb. Ecol. 87, 113–138. https://doi.org/10.3354/ame01973.
Takeuchi, M., Katayama, T., Yamagishi, T., Hanada, S., Tamaki, H., Kamagata, Y., Oshima, K., Hattori, M., Marumo, K., Nedachi, M., Maeda, H., Suwa, Y., Sakata, S., 2014. *Methyloceanibacter caenitepidi* gen. Nov., sp. nov., a facultatively methylotrophic bacterium isolated from marine sediments near a hydrothermal vent. Int. J. Syst. Evol. Microbiol. 64, 462–468. https://doi.org/10.1099/ijs.0.053397-0.
Tamburini, E., Doni, L., Lussu, R., Meloni, F., Cappai, G., Carucci, A., Casalone, E., Mastromei, G., Vitali, F., 2020. Impacts of anthropogenic pollutants on benthic prokaryotic communities in Mediterranean touristic ports. Front. Microbiol. 11, 1234 https://doi.org/10.3389/fmicb.2020.01234.
Torsten, H., Zeileis, A., Millo, G., Mitchell, D., 2012. "R package lmtest: Testing Linear Regression Models" (2012).
Turon, M., Cáliz, J., Garate, L., Casamayor, E.O., Uriz, M.J., 2018. Showcasing the role of seawater in bacteria recruitment and microbiome stability in sponges. Sci. Rep. 8, 15201 https://doi.org/10.1038/s41598-018-33545-1.
Utermann, C., Blümel, M., Busch, K., Buedenbender, L., Lin, Y., Haltli, B.A., Kerr, R.G., Briski, E., Hentschel, U., Tasdemir, D., 2020. Comparative microbiome and metabolome analyses of the marine tunicate *Ciona intestinalis* from native and invaded habitats. Microorganisms 8, 2022. https://doi.org/10.3390/microorganisms8122022.
Vez-Garzón, M., Giménez, J., Sánchez-Márquez, A., Montalvo, T., Navarro, J., 2023. Changes in the feeding ecology of an opportunistic predator inhabiting urban environments in response to COVID-19 lockdown. R. Soc. Open Sci. 10, 221639 https://doi.org/10.1098/rsos.221639.
Villela, H., 2020. Microbiome flexibility provides new perspectives in coral research. BioEssays. https://doi.org/10.1002/bies.202000088.
Vitorino, I.R., Klimek, D., Calusinska, M., Lobo-da-Cunha, A., Vasconcelos, V., Lage, O. M., 2022. *Stieleria sedimenti* sp. nov., a novel member of the family with antimicrobial activity isolated in Portugal from brackish sediments. Microorganisms 10. https://doi.org/10.3390/microorganisms10112151.
Walesiak, M., Dudek, A., Dudek, M., 2014. clusterSim: Searching for optimal clustering procedure for a data set. http://CRAN.R-project.org/package=clusterSim.

Walsh, J.R., Carpenter, S.R., Vander Zanden, M.J., 2016. Invasive species triggers a massive loss of ecosystem services through a trophic cascade. Proc. Natl. Acad. Sci. U. S. A. 113, 4081–4085. https://doi.org/10.1073/pnas.1600366113.

Wang, H., Yang, B., Li, X., Li, Q., Liu, S., 2021. Screening of bacterial pathogens associated with mass summer mortality of the Pacific oyster, *Crassostrea gigas*, in China. Aquac. Rep. 20, 100672 https://doi.org/10.1016/j.aqrep.2021.100672.

Wang, Y., Stingl, U., Anton-Erxleben, F., Geisler, S., Brune, A., Zimmer, M., 2004. "*Candidatus hepatoplasma crinochetorum*," a new, stalk-forming lineage of Mollicutes colonizing the midgut glands of a terrestrial isopod. Appl. Environ. Microbiol. 70, 6166–6172. https://doi.org/10.1128/AEM.70.10.6166-6172.2004.

Wei, J., Zhang, J., Lu, Q., Ren, P., Guo, X., Wang, J., Li, X., Chang, Y., Duan, S., Wang, S., Yu, H., Zhang, X., Yang, X., Gao, H., Dong, B., 2020. Genomic basis of environmental adaptation in the leathery sea squirt (*Styela clava*). Mol. Ecol. Resour. 20, 1414–1431. https://doi.org/10.1111/1755-0998.13209.

Wickham, H., Chang, W., Wickham, M.H., 2016. Package "ggplot2." Create elegant data visualisations using the grammar of graphics. Version 2, 1–189.

Zamora-Briseño, J.A., Cerqueda-García, D., Hernández-Velázquez, I.M., Rivera-Bustamante, R., Huchín-Mian, J.P., Briones-Fourzán, P., Lozano-Álvarez, E., Rodríguez-Canul, R., 2020. Alterations in the gut-associated microbiota of juvenile Caribbean spiny lobsters *Panulirus argus* (Latreille, 1804) infected with PaV1. J. Invertebr. Pathol. 176, 107457 https://doi.org/10.1016/j.jip.2020.107457.

Zenni, R.D., Lamy, J.-B., Lamarque, L.J., Porté, A.J., 2014. Adaptive evolution and phenotypic plasticity during naturalization and spread of invasive species: implications for tree invasion biology. Biol. Invasions 16, 635–644. https://doi.org/10.1007/s10530-013-0607-8.

Zhang, D., 2018. rsq: R-squared and related measures. R package version.